$G\alpha_q$ signals via Trio RhoGEF to modulate synaptic transmission in a model serotonin motor circuit in *C. elegans*

Pravat Dhakal, Sana Chaudhry, and Kevin M. Collins*

Department of Biology, University of Miami, Coral Gables, FL, United States of America

*To whom correspondence should be addressed. Email: *kevin.collins@miami.edu*

57 pages with 6 Figures, 2 Tables and 3 Movies

Abstract

Activated $G\alpha_q$ signals through Phospholipase-Cβ (PLCβ) and Trio, a Rho GTPase exchange factor (RhoGEF), but how these two effector pathways promote synaptic transmission remains poorly understood. We used the egg-laying behavior circuit of *C. elegans* to determine whether PLCβ and Trio mediate serotonin and $G\alpha_q$ signaling through independent or related biochemical pathways. Using genetic rescue experiments, we find that PLCβ functions in neurons while Trio functions in both neurons and the postsynaptic vulval muscles. While $G\alpha_q$, PLCβ, and Trio RhoGEF mutants all fail to lay eggs in response to serotonin, optogenetic stimulation of the serotonin releasing HSN command neurons restores egg laying only in PLCβ mutants. Vulval muscle Ca^{2+} activity remained in PLCβ mutants but was eliminated in strong $G\alpha_q$ and Trio RhoGEF mutants. Exogenous treatment with Phorbol esters that mimic Diacylglycerol (DAG), a product of PIP_2 hydrolysis, rescued egg-laying circuit activity and behavior defects of $G\alpha_q$ signaling mutants, suggesting both Phospholipase C and Rho signaling promote synaptic transmission and egg-laying via DAG production. DAG has been proposed to activate effectors including UNC-13, however, we find that phorbol esters, but not serotonin, stimulate egg laying in *unc-13* mutants. Together, these results show that serotonin signaling through $G\alpha_q$ and PLCβ modulates UNC-13 activity to promote neurotransmitter release. Serotonin also signals through $G\alpha_q$, Trio RhoGEF, and an unidentified PMA-responsive effector to promote postsynaptic muscle excitability. Thus, the same neuromodulator serotonin can signal in distinct cells and effector pathways to activate a motor behavior circuit.

Introduction

Neurons communicate in circuits via synaptic transmission to initiate, sustain, and terminate behaviors. During neurotransmission, both synaptic vesicles and dense-core vesicles fuse with the presynaptic membrane, releasing neurotransmitters and neuropeptides that activate postsynaptic ion channels and G protein coupled receptors (GPCRs) (Betke et al., 2012; Geppetti et al., 2015). While much has been learned about neurotransmitter signaling pathways through ionotropic receptors, the diversity of GPCRs and their signaling pathways has complicated our understanding of how their signaling exerts changes on cell excitability and behavior. The G protein, $G\alpha_q$, is one of the major G proteins expressed in all excitable cells (Offermanns, 2001; Simon et al., 1991; Wilkie et al., 1992). Activated $G\alpha_q$ signals through PIP_2-specific phospholipase-C β (PLCβ) to generate the second messengers, inositol 1,4,5 trisphosphate (IP_3) and diacylglycerol (DAG). IP_3 activates the IP_3 receptor to release Ca^{2+} from intracellular stores and activate downstream kinases, lipases, and ion channels (Berridge et al., 2000; Huang, 1989; Li et al., 2014; Mujica and Gonzalez, 2011). DAG has been shown to recruit and activate numerous effector proteins including UNC-13 and Protein Kinase C (Ananthanarayanan et al., 2003; Brose and Rosenmund, 2002; Lou et al., 2008; Maruyama and Brenner, 1991; Rozengurt et al., 1997; Silinsky and Searl, 2003; Thore et al., 2005), but whether these or other identified DAG targets function to transduce all forms of $G\alpha_q$ signaling *in vivo* remains an open question.

Genetic studies in the nematode worm *C. elegans* show that $G\alpha_q$ signaling through both PLCβ and Trio, a Rho GTPase Exchange Factor (RhoGEF), promotes synaptic transmission. Whether Trio signaling through Rho similarly promotes DAG and IP_3 production, or instead acts through an independent downstream pathway, is not clear. In worms, $G\alpha_q$ knockouts are lethal while PLCβ or Trio RhoGEF single knockouts show strong defects in neurotransmission that disrupt locomotion and egg-laying behaviors, resembling strong $G\alpha_q$ loss-of-function mutants

52 (Bastiani et al., 2003; Brundage et al., 1996; Hajdu-Cronin et al., 1999; Lackner et al., 1999).
53 Worms missing both PLCβ and Trio RhoGEF phenocopy the larval arrest phenotype of $G\alpha_q$ null
54 mutants, consistent with these two effectors relaying most or all of the relevant $G\alpha_q$ signaling
55 (Williams et al., 2007). Genetic and biochemical studies showed that $G\alpha_q$ activation of Trio and
56 Rho is conserved (Chhatriwala et al., 2007; Rojas et al., 2007), however, it remains unclear how
57 PLCβ and Rho signaling promotes neurotransmitter and neuropeptide release *in vivo*. The larval
58 lethality of $G\alpha_q$ null mutants or PLCβ / Trio RhoGEF double mutants can be rescued by the DAG-
59 mimetic phorbol ester, PMA (Reynolds et al., 2005; Steven et al., 2005; Williams et al., 2007),
60 suggesting $G\alpha_q$ signaling through both PLCβ and Trio may ultimately converge to regulate DAG
61 levels and the activation of downstream effectors. Both PLCβ and Trio RhoGEF promote
62 acetylcholine (ACh) release from motor neurons that control locomotion (Lackner et al., 1999;
63 Miller et al., 1999; Williams et al., 2007), although mutations in Trio RhoGEF cause behavior
64 defects more aligned with a function in dense core vesicle release (Hu et al., 2011). PLCβ is
65 expressed in the nervous system and intestine, while $G\alpha_q$ and Trio show additional postsynaptic
66 expression in muscles (Bastiani et al., 2003; Lackner et al., 1999; Steven et al., 1998; Steven et
67 al., 2005). While re-expression of PLCβ or Trio in neurons rescue the locomotion behavior
68 defects of their mutants (Williams et al., 2007), whether these proteins exclusively function in
69 neurons to regulate egg laying, is an open question.

70 Using genetics, optogenetics, pharmacology, and calcium imaging techniques we have
71 investigated how $G\alpha_q$ signaling through its two effector pathways regulate egg-laying circuit
72 activity and behavior. We find that $G\alpha_q$ signals through PLCβ in the presynaptic neurons while
73 $G\alpha_q$ signals through Trio in both neurons and muscles to promote egg laying. These results
74 clarify that despite $G\alpha_q$ signaling through independent PLCβ and Trio pathways, these effectors
75 may ultimately converge to potentiate DAG levels which promote egg-laying behavior.

MATERIALS AND METHODS

Strains

C. elegans worms were maintained at 20°C on Nematode Growth Medium (NGM) agar plates with *E. coli* OP50 as a source of food as described previously (Brenner, 1974). All behavior assays and fluorescence imaging experiments were performed with age-matched adult hermaphrodites aged 20 – 36 h after the late L4 stage. All strains used in this study are listed in Table 1.

Molecular biology and transgenes

Vulval muscle GCaMP5 strains

Vulval muscle Ca^{2+} activity was recorded using GCaMP5G (Akerboom et al., 2013) which was expressed along with mCherry from the *unc-103e* promoter (Collins and Koelle, 2013), as previously described (Collins et al., 2016; Ravi et al., 2018a). The wild-type reporter strain, LX1918 *vsIs164 [unc-103e::GCaMP5::unc-54 3'UTR + unc-103e::mCherry::unc-54 3'UTR + lin-15(+)] lite-1(ce314) lin-15(n765ts) X* was used as described previously (Collins et al., 2016). LX1918 males were crossed separately into DA823 *egl-30(ad805) I*, MT1434 *egl-30(n686) I*, JT47 *egl-8(sa47) V*, MT1083 *egl-8(n488) V*, KG1278 *unc-73(ce362) I*, LX1226 *eat-16(tm761) I*, CG21 *egl-30(tg26) I*, *him-5(e1490) V*, or KP1097 *dgk-1(nu62) X* hermaphrodites to generate MIA140 *egl-30(ad805) I; vsIs164 lite-1(ce314) lin-15(n765ts) X*, MIA139 *egl-30(n686) I; vsIs164 lite-1(ce314) lin-15(n765ts) X*, MIA109 *egl-8(sa47) V; vsIs164 lite-1(ce314) lin-15(n765ts) X*, MIA288 *egl-8(n488) V; vsIs164 lite-1(ce314) lin-15(n765ts) X*, MIA141 *unc-73(ce362) I; vsIs164 lite-1(ce314) lin-15(n765ts) X,* MIA287 *eat-16(tm761) I; vsIs164 lite-1(ce314) lin-15(n765ts) X*, MIA286 *egl-30(tg26) I; vsIs164 lite-1(ce314) lin-15(n765ts) X* ,and MIA296 *dgk-1(nu62) vsIs164 lite-1(ce314) lin-15(n765ts) X*, respectively. The corresponding gene mutation was confirmed by phenotype, genotype, or both. Presence of *vsIs164* was confirmed observing the mCherry

101 marker, and *lite-1(ce314) X* was confirmed with PCR genotyping. Oligo sequences used for
102 genotyping the corresponding mutations are shown in Table 2.
103
104 **Trio RhoGEF-E transgenes**
105 *Pan-neuronal expression*:
106 The *rab-3* promoter was used to drive expression of GFP alone or with Trio-RhoGEF-E. Briefly,
107 plasmids KG#68 (*rab-3p::GFP*; 15 ng/µl) alone or with KG#281 (*rab-3p:: unc-73e;* 50 ng/µL)
108 were injected into KG1278 *unc-73(ce362) I* (Williams et al., 2007). For behavior experiments,
109 five independent GFP-expressing transgenic lines were used, from which a single transgenic
110 line from each was kept: MIA374 *unc-73(ce362) I*; *keyEx66* (expressing GFP alone) and MIA375
111 *unc-73(ce362) I*; *keyEx67* (expressing GFP and Trio RhoGEF-E). Plasmids KG#281(*rab-*
112 *3p::unc-73e*) and KG#68(*rab-3p::GFP*) were kind gifts from Dr. Kenneth Miller.
113
114 *Pan-muscle expression*
115 Plasmid pKMC33 (*rgs-1p::mCherry*) was digested with NheI/KpnI and ligated with similarly
116 digested pPD96.52 (Fire lab *C. elegans* Vector Kit 1999; 1608: L2534, Addgene) to generate
117 pKMC166 (*myo-3p::mCherry*). Plasmid KG#281 (*rab-3p::unc-73e*) was digested with NheI and
118 KpnI, and the insert was ligated into similarly digested pKMC166 to generate pPD3 (*myo-*
119 *3p::unc-73e*). pKMC166 (15 ng/µL) alone or with pPD3 (50 ng/µL) was injected into KG1278
120 *unc-73(ce362) I* mutants. Five independent mCherry-expressing transgenic lines were used for
121 behavior experiments from which a single transgenic line from each was kept: MIA376 *unc-*
122 *73(ce362) I; keyEx68* (expressing mCherry alone) and MIA377 *unc-73(ce362) I*; *keyEx69*
123 (expressing mCherry + Trio RhoGEF-E).
124
125 Neuron and muscle co-expression

126 Plasmids KG#68 (15 ng/µl; pan-neuronal GFP) or pKMC166 (15 ng/µl; pan-muscle mCherry)
127 alone or with KG#281 (50ng/µl; pan-neuronal *unc-73e*) and pPD3 (50ng/µL; pan-muscle *unc-*
128 *73e*) were injected into KG1278 *unc-73(ce362) I*, generating five independent mCherry(+),
129 GFP(+) transgenic lines for behavior experiments from which a single transgenic line from each
130 was kept: MIA372 *unc-73(ce362); keyEx64* expressing mCherry (muscles) and GFP (neurons)
131 only and MIA373 *unc-73(ce362); keyEx65* expressing GFP (neurons), mCherry (muscles) and
132 TrioRhoGEF-E (both neurons and muscles).
133
134 **PLCβ Transgenes**
135 To generate a control plasmid expressing GFP in neurons, GFP coding sequences were
136 amplified from pJM60 (Moresco and Koelle, 2004) using oligonucleotides RE-GFP-FWD / -REV,
137 digested with NheI / KpnI, and ligated into similarly digested pGP3 bearing the *rgs-1* promoter
138 (Dong et al., 2000), generating pKMC78. An *egl-8* cDNA was used to generate and express a
139 functional GFP fusion protein in neurons. Briefly, oligonucleotides egl-8-cDNA-fwd / -rev were
140 used to amplified *egl-8* coding sequences from a plasmid bearing an *egl-8* cDNA provided by
141 Dr. Kenneth Miller (pKP309). This amplicon was digested with NheI / NcoI and ligated into a
142 similarly digested pPD49.26 plasmid, generating pKMC193. Quickchange mutagenesis with
143 oligonucleotides egl-8-Cterm-NotI-fwd / -rev were used to insert an in-frame NotI site near the 3'
144 end of the *egl-8* cDNA in a divergent region of the coding sequence, generating plasmid
145 pKMC194. Coding sequences for *egl-8* bearing this NotI site were then moved to pKMC78 by
146 digestion of pKMC194 with NheI/NcoI followed by ligation into a similarly digested pKMC78,
147 generating pKMC195. Oligonucleotides NotI-GFP-FWD / -REV were used to amplified GFP
148 coding sequences from pKMC78, digested with NotI, and ligated into a similarly digested
149 pKMC195, generating pKMC196. A strain bearing the *egl-8(sa47)* mutation was generously
150 provided by Dr. Joshua Kaplan and backcrossed four times to N2 wild-type animals to generate

151 LX1225 *egl-8(sa47) V.* MT8189 *lin-15(n765ts)* males were mated to LX1225 to generate LX1287
152 *egl-8(sa47) V; lin-15(n765ts) X* hermaphrodites that were kept at 15°C prior to injection.
153 Plasmids expressing GFP alone (pKMC78; 5 ng/µl) or *egl-8* CDNA fused to GFP (pKMC196; 5
154 ng/µl) were injected along with pL15EK (50ng/µl) into LX1287 hermaphrodites. For behavior
155 experiments, five independent GFP-expressing lines were used from which a single transgenic
156 line (*vsEx679* [GFP] and *vsEx680* [EGL-8::GFP], respectively) was kept.
157

158 **Vulval muscle Channelrhodopsin-2 strains**

159 N2 males were crossed into MIA229 *keyIs48 [ceh-24p::ChR2::unc-54 3'UTR + lin-15(+)], lite-*
160 *1(ce314), lin-15(n765ts) X* (Kopchock et al., 2021) to produce F1 heterozygous males, which
161 then were crossed separately into MIA211 *unc-73(ce362) I; lite-1(ce314) lin-15(n765ts) X,*
162 MIA299 *egl-30(ad805) I; lite-1(ce314) lin-15(n765ts) X*, MIA303 *egl-8(n488) V; lite-1(ce314) lin-*
163 *15(n765ts) X*, or MIA307 *egl-8(sa47) V; lite-1(ce314) lin-15(n765ts) X* hermaphrodites to
164 generate vulval muscle specific Channelrhodopsin-2 (ChR2) expressing transgenic lines
165 MIA248 *unc-73(ce362) I; keyIs48; lite-1(ce314) X*, MIA301 *egl-30(ad805) I; keyIs48; lite-*
166 *1(ce314) X*, MIA305 *egl-8(n488) V; keyIs48; lite-1(ce314) X*, and MIA309 *egl-8(sa47) V;*
167 *keyIs48; lite-1(ce314) X*. The presence of *lite-1(ce362)* was confirmed by genotyping as above,
168 and the presence of the ChR2 transgene was confirmed by rescue of the *lin-15(n765ts)* multi-
169 vulva (Muv) phenotype.
170

171 **HSN Channelrhodopsin strains**

172 ChR2 was expressed in the HSNs from the *egl-6* promoter via an integrated transgene (Emtage
173 et al., 2012). This transgene was crossed into $G\alpha_q$ signaling mutants as follows. N2 males were
174 crossed into LX1836 *wzIs30 IV; lite-1(ce314) lin-15(n765ts) X* to generate heterozygous F1
175 males, which were then crossed separately into MIA211 *unc-73(ce362) I; lite-1(ce314) lin-*

176 *15(n765ts) X,* MIA299 *egl-30(ad805) I; lite-1(ce314) lin-15(n765ts) X*, MIA303 *egl-8(n488) V;*
177 *lite-1(ce314) lin-15(n765ts) X,* or MIA307 *egl-8(sa47) V; lite-1(ce314) lin-15(n765ts) X*
178 hermaphrodites to generate MIA247 *unc-73(ce362) I; wzIs30 IV; lite-1(ce314) X,* MIA300 *egl-*
179 *30(ad805) I; wzIs30 IV; lite-1(ce314) X*, MIA304 *wzIs30 IV; egl-8(n488)V; lite-1(ce314) X*, and
180 MIA308 *wzIs30 IV; egl-8(sa47) V; lite-1(ce314) X*. The presence of *lite-1(ce362)* was confirmed
181 by PCR genotyping, and the *wzIs30* transgene was confirmed by rescue of the *lin-15(n765ts)*
182 Muv phenotype.
183
184 **Behavior assays**
185 Quantification of egg accumulation was performed as described (Chase et al., 2004). Staged
186 adults were obtained by picking late L4 animals and culturing them 24-30hr at 20°C. Each animal
187 was placed in 7 µL of 20% hypochlorite (bleach) solution and eggs were counted after animals
188 had dissolved. Numbers of eggs and any internally hatched L1 animals were combined.
189
190 **Pharmacological assays**
191 Egg laying in response to exogenous serotonin was performed as described (Banerjee et al.,
192 2017). Individual staged adult animals were placed in 100 µl of either M9 buffer alone, or M9
193 containing 7.5 mg/ml serotonin (creatinine sulfate monohydrate salt, Sigma-Aldrich #H7752) or
194 M9 containing 10 µM PMA (Phorbol-12-myristate-13-acetate, Calbiochem #524400) in a 96-well
195 microtiter dish. After 1 hour, the number of released eggs and L1 larvae in each well were
196 counted. Since egg-laying defective animals sometimes release one or two progeny in response
197 to mechanical stimulation when they are first picked into the well, animals were only were
198 recorded as responding if they laid 3 or more progeny. For calcium imaging, NGM plates
199 containing PMA or control (equivolume ethanol solvent) were prepared as described (Reynolds
200 et al., 2005). Age-matched adult worms (n>10) from each genotype were placed on separate

201 PMA or control NGM plates at room temperature for 2 h, and subsequently transferred onto an
202 agar chunk which was placed between the glass slide and a glass cover slip for Ca^{2+} activity
203 recording (Ravi et al., 2018b). The unused plates were kept at 4 °C for future use.
204
205 **Optogenetic assay**
206 All-*trans* retinal (Sigma Aldrich, R2500) was resuspended in ethanol (100%) to make 100 mM
207 solution and added to a warmed culture of OP50 bacteria grown in B Broth media to a final
208 concentration of 0.4 mM. Individual NGM agar plates were seeded with 200 µl of freshly
209 prepared +ATR food, and were grown in the dark for ~24 hours prior to use. In all photo-
210 stimulation experiments, control animals were grown in the absence of ATR. Animals were
211 exposed to blue light using a Leica M165FC stereomicroscope equipped with an EL6000 metal
212 halide light source generating 8–16 mW/cm^2 (depending on the magnification used) of ~470 ±
213 20 nm blue light through a GFP filter. The 30 s on/off sequence was programmed and controlled
214 using the Optogenetics TTL Pulse Generator (OTPG-4, Version 3.3) triggering a SHB1 series
215 shutter controller (ThorLabs; 170712-1).
216
217 **Microscopy**
218 **Ratiometric Ca^{2+} imaging**
219 Vulval muscle Ca^{2+} activity was performed in freely behaving adult animals at 24-30 h past the
220 late L4 larval stage, as described previously (Collins and Koelle 2013; Collins *et al.* 2016; Ravi
221 *et al.* 2018a). Worms co-expressing GCaMP5G and mCherry under the *unc-103e* promoter
222 transgene *vsIs164* were mounted beneath the chunk of agar over the glass slide. Ca^{2+} activity
223 was recorded through an 20X Apochromatic objective (0.8 NA) mounted on an inverted Zeiss
224 Axio Observer.Z1. A Colibri.2 LED illumination system was used to excite GCaMP5 at 470 nm
225 and mCherry at 590 nm for 10 msec every 50 msec. GFP and mCherry fluorescence emission

226 channels were separated using a Hamamatsu W-VIEW Gemini image splitter and recorded
227 simultaneously for 10 min with an ORCA-Flash 4.0 V2 sCMOS camera at 256 / 256-pixel
228 resolution (4x4 binning) at 16-bit depth. The motorized stage was manually controlled using a
229 joystick to maintain the freely behaving animal in the field of view. Image sequences were
230 exported to Volocity software (Quorum Technologies Inc.) for segmentation and ratiometric
231 analysis. Ca^{2+} transient peaks from ratio traces were detected using a custom MATLAB script,
232 as described (Ravi *et al.* 2018a).
233

234 **Experimental design and statistical analysis**

235 Sample sizes for behavioral assays followed previous studies (Chase et al., 2004; Collins et al.,
236 2016). Statistical analysis was performed using Prism 8 (GraphPad). Ca^{2+} transient peak
237 amplitudes, widths, and inter-transient intervals were pooled from multiple animals (typically ≥
238 10 animals per genotype). All statistical tests were corrected for multiple comparisons
239 (Bonferroni for one-way ANOVA or Fisher's exact; Dunn for Kruskal–Wallis). Each figure legend
240 indicates individual p-values.
241
242

243 **Results**

244 **Trio RhoGEF acts both in neurons and muscle to drive egg-laying behavior**

245 Prior work has shown that $G\alpha_q$ signaling (Fig. 1A) through PLCβ and Trio RhoGEF promotes
246 neurotransmitter release and locomotion (Brundage et al., 1996; Miller et al., 1999; Williams et
247 al., 2007), however, whether $G\alpha_q$ and its effectors similarly regulate other *C. elegans* behavior
248 circuits is less well established. To address this uncertainty, we chose to examine the neural
249 circuit driving egg-laying behavior (Fig. 1B). Egg-laying behavior in *C. elegans* is regulated by
250 small motor circuit with defined neurons and muscle connectivity (Cook et al., 2019; White et al.,
251 1986). The HSNs are serotonergic command motor neurons (Fig. 1B) that initiate the egg-laying
252 active state and promote the excitability of the vm1 and vm2 egg-laying vulval muscles
253 (Waggoner et al. 1998; Emtage et al. 2012; Collins et al. 2016) while innervating ventral cord
254 neurons release acetylcholine to regulate muscle contraction (Kim et al., 2001; Kopchock et al.,
255 2021; Waggoner et al., 2000a). We first examined the steady-state accumulation of eggs in the
256 uterus as a proxy for changes in egg-laying circuit activity and behavior. As previously shown,
257 animals bearing mutations in the EAT-16 RGS protein, which inhibits $G\alpha_q$ signaling (Hajdu-
258 Cronin et al., 1999), or gain-of-function mutations in $G\alpha_q$ itself, (Doi and Iwasaki, 2002) showed
259 a significant increase in egg laying resulting in a significant reduction in egg accumulation
260 compared to the ~12 ± 3 embryos retained in wild-type animals (Fig. 1C-E; Fig. 1I). Conversely,
261 animals bearing mutations which reduce $G\alpha_q$ signaling through its effectors showed the opposite
262 phenotype. Animals bearing an early nonsense mutation predicted to be a PLCβ null mutant,
263 [*egl-8(sa47)*], (Lackner et al., 1999; Williams et al., 2007) accumulated an average of 21 eggs,
264 a significant increase (Fig. 1G). Animals bearing a missense mutation in the RhoGEF domain of
265 Trio, *unc-73(ce362)* (Williams et al., 2007), showed an even stronger increase in egg
266 accumulation, accumulating 31 eggs and closely resembling animals bearing loss-of-function

267 mutations in $G\alpha_q$ itself (Fig. 1F-1I). Together, these results confirm that $G\alpha_q$ and its effectors
268 PLCβ and Trio RhoGEF are required for egg-laying behavior in *C. elegans* and that loss of the
269 Trio RhoGEF branch causes a stronger behavior impairment compared to loss of PLCβ.
270
271 Previous work has shown that PLCβ is expressed in neurons and in the intestine while $G\alpha_q$ and
272 Trio are expressed in nearly all excitable cells including neurons and muscles (Bastiani et al.,
273 2003; Brundage et al., 1996; Lackner et al., 1999; Miller et al., 1999; Steven et al., 1998). To
274 understand where $G\alpha_q$ and its effectors function to regulate egg laying, we used cell-specific
275 promoters to express cDNAs encoding PLCβ or Trio RhoGEF in either all neurons, in the body
276 wall and egg-laying vulval muscles, or in both neurons and muscles. We found that transgenic
277 expression of PLCβ from a neuron-specific promoter in PLCβ null mutants was sufficient to
278 rescue their defects in egg laying (Fig. 1J) and acetylcholine (ACh) release as measured by
279 restoration of sensitivity to aldicarb, a cholinesterase inhibitor (data not shown). Previous work
280 has indicated the presence of eight transcript variants of Trio (A, B, C1, C2, D1, D2, E, and F),
281 which are differentially expressed in *C. elegans* (Steven et al., 1998; Steven et al., 2005).
282 Transgenic expression of Trio RhoGEF-E in neurons is fully sufficient to rescue the locomotion
283 defects of Trio RhoGEF mutants (Williams et al., 2007). To explore whether Trio RhoGEF acts
284 similarly in neurons for egg laying, we used a pan-neuronal promoter to express Trio RhoGEF-
285 E and measured egg accumulation in these animals. We observed a partial, but significant
286 reduction in the number of eggs retained in Trio RhoGEF mutants (~36 eggs) compared to
287 control Trio mutant animals (~42 eggs; Fig. 1K). In contrast, transgenic expression of Trio
288 RhoGEF-E in the egg-laying vulval muscles from a muscle-specific promoter showed a much
289 greater rescue of egg accumulation (~25 eggs), and this rescue of egg laying was improved to
290 nearly wild-type levels when Trio RhoGEF was expressed in both neurons and muscles (~19
291 eggs; Fig. 1K). Together, these results confirm that $G\alpha_q$ signals through both PLCβ and Trio

292 RhoGEF function in neurons to regulate egg-laying behavior. Our results also suggest the $G\alpha_q$
293 effector Trio also functions in the postsynaptic vulval muscles for proper regulation of egg laying,
294 a finding consistent with previously results regarding $G\alpha_q$ (Bastiani et al., 2003).
295
296 **Serotonin signals through $G\alpha_q$, Trio, and PLCβ to promote egg laying.**
297 Previous studies have shown that serotonin released from the HSNs signals through G-protein
298 coupled serotonin receptors expressed on the vulval muscles (Bastiani et al., 2003; Dempsey et
299 al., 2005; Fernandez et al., 2020; Tanis et al., 2008; Xiao et al., 2006). The vulval muscles are
300 also innervated by cholinergic ventral cord motor neurons (Cook et al., 2019; White et al., 1986)
301 whose release of ACh is regulated by serotonin and G protein signaling (Nurrish et al., 1999).
302 To test whether serotonin promotes egg laying by activating receptors that couple to $G\alpha_q$, we
303 measured how serotonin signaling from the HSNs drives egg laying in $G\alpha_q$ signaling mutants.
304 Serotonin promotes egg laying in hypertonic M9 buffer, a condition that normally inhibits egg
305 laying in both wild-type and HSNs-deficient *egl-1(dm)* mutants, which developmentally lack the
306 HSNs (Fig. 2B). Consistent with the previous results (Bastiani et al., 2003; Brundage et al., 1996;
307 Trent et al., 1983), nearly 78% of wild-type and 70% of HSN-deficient *egl-1(dm)* animals laid
308 eggs in response to serotonin compared to only 13% of mutant animals lacking $G\alpha_q$ (Fig. 2B).
309 Serotonin response was similarly and significantly reduced to 23% and 3% in PLCβ and Trio
310 RhoGEF mutant animals, respectively (Fig. 2B). The distinct responses of animals without HSNs
311 and animals lacking $G\alpha_q$ signaling indicate that $G\alpha_q$, PLCβ and Trio act at least in part outside
312 of HSNs to promote egg laying in response to exogenous serotonin. To determine where Trio
313 RhoGEF deficiency caused serotonin insensitivity, we measured egg laying in animals
314 expressing Trio RhoGEF in either neurons, muscles, or both. Transgenic expression of Trio
315 RhoGEF in neurons failed to rescue egg laying in response to serotonin (Fig. 2C), but expression

316 of Trio RhoGEF in muscles, or in both neurons and muscles, restored egg laying to of animals
317 (Fig. 2C), suggesting Trio mediates vulval muscle serotonin signaling. Together, these results
318 indicate that $G\alpha_q$, PLCβ and Trio RhoGEF function outside of the HSNs to drive egg laying in
319 response to serotonin. The fact that PLCβ mutants are resistant to serotonin but unlike Trio
320 mutants, show hyperactive egg-laying behavior upon pan-neuronal overexpression, suggests
321 PLCβ acts presynaptically, either downstream or parallel to the HSNs, possibly to regulate ACh
322 release, while Trio RhoGEF functions downstream of HSN, likely functioning postsynaptically in
323 the egg-laying vulval muscles.
324
325 **Optogenetic stimulation of the HSNs and vulval muscles suggests cellular specificity of**
326 **$G\alpha_q$ effectors for egg-laying.**
327 Optogenetic stimulation of Channelrhodopsin-2 (ChR2) expressed in either the HSNs (Emtage
328 et al., 2012) or vulval muscles (Kopchock et al., 2021) can drive egg laying. To test whether and
329 how $G\alpha_q$ and its effectors signal downstream to mediate this response, we expressed ChR2 in
330 HSNs in $G\alpha_q$ and effector mutants and measured egg laying during 30s of exposure to blue light.
331 Blue light stimulation of the HSNs drove the release of ~3 eggs in wild-type animals, which was
332 reduced to essentially zero in $G\alpha_q$ [(*egl-30(ad805)*] and Trio RhoGEF [*unc-73(ce362)*] mutants
333 (Fig. 3A), consistent to our previous results showing Trio RhoGEF acts downstream of the HSNs
334 in the postsynaptic vulval muscles. In contrast, stimulation of the HSNs in PLCβ null mutants
335 [*egl-8(sa47)* and *egl-8(nu488)*] drove egg release, releasing ~4 and ~6 embryos respectively in
336 30 s (Fig. 3A). To test whether the failure of egg laying in $G\alpha_q$ and Trio RhoGEF mutants was
337 caused by developmental defects in the circuit, rather than excitability deficits, we expressed
338 and stimulated ChR2 in the vulval muscles. Blue light exposure drove the release of ~4 eggs in
339 30 s in wild-type animals. Both PLCβ [*egl-8(sa47)* and *egl-8(nu488)*] and Trio RhoGEF mutants

340 [*unc-73(ce362)*] laid a similar number of eggs as wild-type control animals after blue light
341 stimulation (Fig. 3B). The *egl-30(ad805)* $G\alpha_q$ mutant laid slightly fewer eggs (~3) but this was
342 not significantly different than wild type. Thus, the failure of $G\alpha_q$ and Trio mutants to lay eggs in
343 response to exogenous serotonin or optogenetic stimulation of the HSNs does not arise from
344 some intrinsic defect in vulval muscle contractility, but rather a specific deficiency in muscle
345 electrical excitability. These results support the conclusion from our rescue experiments (Fig.
346 1J-1K) that $G\alpha_q$ signals through PLCβ and Trio RhoGEF in distinct cells and through unique
347 mechanisms to promote egg-laying circuit activity and behavior.
348

349 **$G\alpha_q$ and Trio are required for vulval muscle Ca^{2+} activity**

350 Egg laying in *C. elegans* is a two-state behavior where ~20 minute inactive states are punctuated
351 by ~2-minute active states with high levels of Ca2+ activity in the egg-laying circuit driving
352 release of 3-5 eggs (Collins et al., 2016; Waggoner et al., 1998). Loss of $G\alpha_q$ signaling in *egl-*
353 *30(n686)* animals causes a significant reduction in spontaneous and serotonin-induced vulval
354 muscle Ca^{2+} transients in immobilized animals (Shyn et al., 2003). We therefore tested whether
355 these $G\alpha_q$ dependent Ca^{2+} activity defects were shared in PLCβ and Trio RhoGEF mutants. We
356 expressed the genetically encoded Ca^{2+} reporter, GCaMP5, along with mCherry in the vulval
357 muscles of animals with either increased or decreased $G\alpha_q$ signaling and performed ratiometric
358 imaging in freely behaving animals. As shown in Figure 4A, the normal two-state pattern of vulval
359 muscle Ca^{2+} activity is lost in animals bearing strong loss-of-function $G\alpha_q$ or Trio RhoGEF
360 mutations. In both the *egl-30(ad805)* $G\alpha_q$ and *unc-73(ce362)* Trio mutants, we failed to observe
361 either the strong egg-laying Ca^{2+} transients where both the vm1 and vm2 muscles contract or
362 even the smaller amplitude rhythmic 'twitch' Ca^{2+} transients that are localized to the vm1 muscles
363 (Fig. 4A), strongly reducing the observed Ca^{2+} transient frequency (Fig. 4B). In contrast, the

364 weaker *egl-30(n686)* $G\alpha_q$ mutant and two different PLCβ null mutants showed grossly normal
365 vulval muscle Ca^{2+} activity during both egg-laying and twitch transients (Fig. 4A-C). The elevated
366 pattern of vulval muscle Ca^{2+} activity in weak *egl-30(n686)* $G\alpha_q$ and PLCβ mutants we observed
367 resembled *egl-1(dm)* animals lacking the HSNs (Collins et al., 2016). These animals still enter
368 and leave infrequent egg-laying active states, possibly driven by the accumulation of eggs in the
369 uterus (Ravi et al., 2018a). DAG Kinase-θ (DGK-θ) is thought to reduce DAG signaling through
370 conversion to phosphatidic acid (Fig. 1A). Loss of the DGK-θ/DGK-1 increases neurotransmitter
371 release and egg laying, likely through elevation of DAG levels and activation of downstream
372 effectors (Jose and Koelle, 2005; Miller et al., 1996; Nurrish et al., 1999). To test if *dgk-1* mutants
373 have increased egg-laying muscle activity, we performed Ca^{2+} imaging in *dgk-1(nu62)* mutants.
374 Somewhat surprisingly, DAG Kinase mutant animals did not show a significant increase in vulval
375 muscle Ca^{2+} activity (Fig. 4A-C). Like PLCβ, DGK-1 is expressed in neurons (Nurrish et al.,
376 1999), suggesting alterations of IP_3 and /or DAG levels in neurons may affect the frequency of
377 egg-laying active states without altering the overall pattern or strength of vulval muscle Ca^{2+}
378 activity within those active states. Conversely, animals with increased $G\alpha_q$ signaling either from
379 a gain-of-function *egl-30(tg26)* mutations or *eat-16(tm761)* null mutations showed a significant
380 increase in the amplitude of vulval muscle Ca^{2+} transients (Fig. 4B and 4C). There was also an
381 increase in the frequency of vulval muscle Ca^{2+} transients in *egl-30(tg26)* mutants, but this effect
382 did not rise to the level of significance in *eat-16(tm761*) mutants. Together, these results indicate
383 $G\alpha_q$ signaling through Trio RhoGEF, but not PLCβ, promotes vulval muscle activity that drives
384 twitching and egg-laying Ca^{2+} transients during egg-laying active states.
385
386 **DAG mimetics restore muscle activity and egg laying to $G\alpha_q$ signaling mutants**

387 How does serotonin signaling through $G\alpha_q$ promote vulval muscle activity? Previous results have
388 shown that DAG mimetic Phorbol esters restore locomotion and animal viability to $G\alpha_q$ null
389 mutants and to PLCβ, Trio RhoGEF double mutants (Williams et al., 2007). However, whether
390 phorbol esters rescued egg-laying behavior in $G\alpha_q$ or effector single mutants was not reported,
391 raising questions as to whether $G\alpha_q$ rescue by phorbols esters was a general feature or was
392 restricted to specific effector signaling pathways or behaviors (Fig. 5A). We measured the egg-
393 laying responses of wild-type animals and $G\alpha_q$ signaling mutants to Phorbol 12-myristate 13-
394 acetate (PMA). As shown in Figure 5B, PMA treatment strongly stimulated egg laying in wild-
395 type animals and all mutants with reduced $G\alpha_q$ signaling (≥80% animals laying eggs). Like
396 serotonin (Fig. 2B), PMA also rescued egg laying in *egl-1(dm)* mutant animals lacking the HSNs
397 (Fig. 4B), but only PMA rescued egg laying in $G\alpha_q$ and effector signaling mutants. These results
398 are consistent with PMA acting downstream of both serotonin release from the HSNs and its
399 subsequent signaling through $G\alpha_q$. We next imaged how exogenous PMA affected vulval muscle
400 Ca^{2+} activity. We performed 10-minute GCaMP5 recordings of wild-type or $G\alpha_q$ signaling
401 mutants treated for two hours with 10 μM PMA (Movies 1-3). Quantitation of Ca^{2+} transients
402 showed that exogenous PMA increased vulval muscle Ca^{2+} activity in wild-type animals, as
403 shown by the more frequent rhythmic twitch Ca^{2+} transients (Movie 1). PMA also restored both
404 rhythmic twitch and egg-laying Ca^{2+} transients to strong $G\alpha_q$ and Trio RhoGEF signaling
405 mutants, as measured by both an increase in Ca^{2+} transient peak amplitude and frequency (Fig.
406 5C-5E). While PMA treatment did not restore vulval muscle Ca^{2+} transient frequency in $G\alpha_q$ and
407 Trio mutants to wild-type levels, Ca^{2+} transient frequency was significantly improved in $G\alpha_q$
408 mutant animals (Fig. 5C-5D). We did record more Ca^{2+} transients in Trio mutants after treatment
409 with PMA, but there was no significant difference to the vehicle control. We interpret differences
410 observed in PMA rescue of egg laying (Fig. 5B) and vulval muscle Ca^{2+} (Fig. 5C-D) as being a

411 result of the shortness of the 10-minute Ca^{2+} recording period that followed PMA treatment. Egg-
412 laying active states typically occur every ~20 minutes in wild-type animals (Waggoner et al.,
413 1998) and every 12-15 minutes in hyperactive egg-laying behavior mutants that resemble the
414 effects of PMA treatment (Ravi et al., 2020; Waggoner et al., 2000b). The M9 buffer assays allow
415 egg-laying events to accumulate over one hour without having to capture specific events. While
416 we did observe nearly all $G\alpha_q$ and Trio mutant animals as now being able to lay eggs, this was
417 not always captured during the Ca^{2+} recording. Together, these studies show that DAG-mimetic
418 phorbol esters restore muscle contractility defects of $G\alpha_q$ and Trio RhoGEF mutants, suggesting
419 DAG production is a major and necessary consequence of $G\alpha_q$ signaling.
420

421 **DAG promotes egg laying independent of UNC-13 and Protein Kinase C**

422 How do Phorbol esters such as PMA rescue vulval muscle Ca^{2+} activity and egg laying? Previous
423 results have shown that DAG and PMA binds to C1 domain-containing proteins such as mUNC-
424 13/UNC-13 and Protein Kinase C (PKC) to regulate their activity (Betz et al., 1998; Huang, 1989;
425 Konig et al., 1985; Newton, 2001; Silinsky and Searl, 2003).To test if DAG regulates egg-laying
426 behavior through activation of UNC-13 or PKC, we tested how PMA and serotonin affect egg
427 laying in mutants lacking these proteins (Fig. 6). Mutants that eliminate axonal and synaptic
428 UNC-13 show reduced egg laying, accumulating an average of 22 eggs compared to 15 seen in
429 wild-type animals (Fig. 6A). Null *unc-13(s69)* and loss of function *unc-13(e51)* mutants have
430 much less severe egg-laying defects compared to $G\alpha_q$ signaling mutants, accumulating ~22 and
431 ~19 eggs (Fig. 6A) compared to >30 eggs (Fig. 1C-I). These results suggest that $G\alpha_q$ promotes
432 synaptic transmission and egg-laying through an UNC-13 independent pathway. If PMA
433 activation of vulval muscle Ca^{2+} and egg laying were mediated by UNC-13, then mutations that
434 eliminate this protein should reduce that response. However, *unc-13* mutants still laid eggs in

435 response to PMA (Fig. 6B). Because DAG production may be a conserved biochemical
436 consequence of $G\alpha_q$ signaling through both PLCβ and Trio RhoGEF pathways, and both effector
437 pathways have functions in neurons, we hypothesized that serotonin might promote egg laying
438 via modulation of UNC-13 activity. In support of this model, *unc-13* mutants failed to lay eggs in
439 response to serotonin (Fig. 6B). To determine whether $G\alpha_q$ promotes egg laying through Protein
440 Kinase C, we analyzed egg accumulation in animals bearing predicted null mutations in different
441 PKC isoforms (Edwards et al., 2012; Hyde et al., 2011; Okochi et al., 2005; Tabuse, 2002;
442 Tabuse et al., 1989). PKC-1 has previously been shown to promote neuropeptide transmission
443 (Sieburth et al., 2007). While neuropeptides signal to promote egg laying (Avery et al., 1993;
444 Brewer et al., 2019; Jacob and Kaplan, 2003; Kass et al., 2001), PKC-1 (nPKC-ε) null mutants
445 showed a grossly normal egg accumulation of 14~17 eggs (Fig. 6C). Animals bearing predicted
446 null mutants of novel and conventional PKCs such as nPKCδ/θ (TPA-1) and cPKCα/β (PKC-2)
447 orthologs also show no significant differences in egg accumulation (Fig. 6C), suggesting that
448 disruption of PKC signaling does not strongly affect egg-laying behavior. Like UNC-13, If PMA
449 activation of vulval muscle Ca^{2+} and egg laying were mediated by PKCs, then mutations that
450 eliminate PKCs, should reduce that response. However, PKC mutant animals still laid eggs in
451 response to PMA (Fig. 6C) suggesting PKCs do not mediate the egg-laying response to PMA.
452 Together, these results show that serotonin signals through $G\alpha_q$ via UNC-13 to promote
453 neurotransmitter release, however, there are additional targets of DAG that function in parallel
454 to UNC-13 in neurons and/or downstream of UNC-13 in the vulval muscles to promote egg
455 laying.
456

457 **Discussion**

458 In this study we demonstrated the cellular specificity of $G\alpha_q$ signaling as it regulates egg-laying
459 circuit activity and behavior using molecular genetics, optogenetics, pharmacology, and calcium
460 imaging techniques. We found that $G\alpha_q$ effectors PLCβ and Trio RhoGEF differentially act in
461 neurons and muscles to promote synaptic transmission and egg-laying behavior. PLCβ signals
462 presynaptically in neurons while Trio signals both presynaptically in neurons and
463 postsynaptically in muscles. Although $G\alpha_q$, PLCβ, and Trio mutants all fail to lay eggs in
464 response to serotonin, optogenetic stimulation of HSNs fully rescued egg laying in PLCβ but not
465 $G\alpha_q$ or Trio RhoGEF mutants, suggesting hyperactivation of the HSNs may be able to bypass
466 PLCβ signaling in some cases. Recent work has shown that the HSNs releases NLP-3
467 neuropeptides which can promote egg laying even in *tph-1* mutants lacking serotonin (Brewer
468 et al., 2019). Because pan-neuronal expression of PLCβ was able to rescue both egg-laying and
469 cholinergic transmission defects of PLCβ null mutants, we propose that $G\alpha_q$ signals through
470 PLCβ to promote acetylcholine release from the VA, VB, and VC neurons, which also innervate
471 the vulval muscles alongside the HSNs (Cook et al., 2019; White et al., 1986). Consistent with
472 this model, we have recently shown that VC synaptic transmission is important for egg laying in
473 response to serotonin (Kopchock et al., 2021). Previous studies have shown that Trio acts in the
474 presynaptic motor neurons to regulate locomotion behavior (Hu et al., 2011; Steven et al., 2005;
475 Williams et al., 2007). Our studies show that Trio overexpression in either neurons or muscles
476 alone is insufficient to restore wild-type level of egg-laying behavior, but expression in both is
477 sufficient. These results further indicate that $G\alpha_q$ signaling through PLCβ and Trio RhoGEF fulfill
478 distinct functions during locomotion and egg-laying behaviors.
479

480 How do $G\alpha_q$, PLCβ and Trio-RhoGEF signaling promote egg-laying behavior? Earlier
481 studies have suggested that Rho ortholog RHO-1 in *C. elegans* regulates synaptic activity in a
482 mechanism that involves the G12 family protein GPA-12 (Hiley et al., 2006; Lutz et al., 2005).
483 Activated RHO-1 also directly binds to and inhibits the DGK-1 diacylglycerol kinase expressed
484 in neurons that signals to reduce DAG available to bind effectors (Hiley et al., 2006; McMullan
485 et al., 2006). Our data demonstrate that $G\alpha_q$ signaling regulates postsynaptic vulval muscle
486 activity mainly through $G\alpha_q$-Trio pathway as $G\alpha_q$, and Trio mutants show a similarly strong
487 reduction in vulval muscle Ca^{2+} activity. Because muscle activity defects in $G\alpha_q$ and Trio mutants
488 can be restored by the DAG-mimetic PMA, we suggest that insufficient levels of DAG are
489 responsible for the circuit activity and behavior defects of $G\alpha_q$ and Trio RhoGEF mutants. In the
490 absence of PLCβ, how would parallel $G\alpha_q$ signaling through Trio RhoGEF and RHO-1 generate
491 DAG? Besides PLCβ (EGL-8), *C. elegans* expresses four other PLC orthologs: PLCε (PLC-1),
492 PLC-2, PLCγ (PLC-3), and PLCδ (PLC-4) (Vázquez-Manrique et al., 2008). *In vitro* studies with
493 cultured mammalian cells show that small G proteins like Rho can bind to and activate PLCε
494 (Seifert et al., 2008; Wing et al., 2003). Genetic evidence in *C. elegans* suggests a model that
495 both PLCε and PLCγ likely function downstream of $G\alpha_q$ to promote cell activity (Kunitomo et al.,
496 2013; Yu et al., 2013), but whether Trio activation of Rho ultimately acts through these PLCs to
497 produce DAG is not clear. One approach to test if these other PLCs mediate Rho signaling would
498 be to perform genetic epistasis experiments. However, loss of Rho-1 causes lethality (Jantsch-
499 Plunger et al., 2000; McMullan and Nurrish, 2011) and loss of PLCε and PLCγ cause sterility
500 defects, limiting our ability to measure differences in egg laying. Imaging or biochemical
501 experiments documenting changes in PIP_2 (Stauffer et al., 1998) and/or DAG (Ohno et al., 2017;
502 Tewson et al., 2012) could allow for directs tests of whether $G\alpha_q$ signaling through Trio and Rho
503 changes PIP2 and DAG levels *in vivo*.

504 Previous studies have shown that the DAG mimetic phorbol esters promote both synaptic
505 vesicle and dense core vesicle release from neurons and neurosecretory cells (Silinsky and
506 Searl, 2003). DAG and phorbol esters activate many effectors including mUNC-13 in the brain
507 and Protein Kinase C (PKC) in nearly all cells (Betz et al., 1998; Huang, 1989). In *C. elegans*,
508 treatment of exogenous PMA promotes hypersensitivity to the paralytic effects of aldicarb
509 (Sieburth et al., 2007). Double mutants of both PKC-1 null and UNC-13 (H17K) show a greater
510 magnitude of resistivity to phorbol esters compared to either mutant alone suggesting that PMA
511 acts in part through these effectors to regulate ACh release (Sieburth et al., 2007; Silinsky and
512 Searl, 2003). Our data show that animals lacking either UNC-13 or single PKC isoforms still
513 show a robust egg-laying response to PMA (Fig. 6), suggesting DAG and PMA promote muscle
514 activity via other targets. *In vitro* studies show ROCK (Rho-associated coiled-coil kinase)
515 activation in PMA-induced apoptosis and macrophage differentiation (Chang et al., 2006; Yang
516 et al., 2017). ROCK has a predicted C1 domain that mediates protein interaction with DAG and
517 might bind and be similarly activated by PMA (Xiao et al., 2009). In *C. elegans,* RHO-1 signals
518 through LET-502/ROCK to phosphorylate non-muscle myosin light chain (Shimizu et al., 2018).
519 $G\alpha_q$ also promotes neurotransmitter release via additional kinase targets including SEK-1
520 Mitogen-Activated Protein Kinase Kinase in the p38 MAPK pathway and KSR-1 in the ERK
521 MAPK pathway (Coleman et al., 2018; Hoyt et al., 2017). KSR-1 is particularly interesting in that
522 its N-terminus shares sequence similarly with C1 domains that might mediate regulation by DAG.
523 Loss of KSR-1 and other ERK MAPK components also suppress the loopy locomotion defects
524 caused by gain-of-function mutations in Rho-1 (Coleman et al., 2018). Taken together, our work
525 is consistent with a model where additional DAG-sensitive effectors act downstream of $G\alpha_q$ to
526 promote muscle contractility during egg laying.

527 Apart from direct activation of C1 domain containing effectors, emerging evidence
528 indicates DAG can regulate neural circuit activity via endocannabinoid-mediated retrograde

529 signaling. In pyramidal cells of the mouse hippocampus, postsynaptic calcium influx through
530 voltage-gated calcium channels activates PLCβ1 to generate DAG (Hashimotodani et al., 2006;
531 Hashimotodani et al., 2007; Soltesz et al., 2015). Diacylglycerol lipase-α (DAGLα) can convert
532 DAG to Arachidonoylglycerol (2-AG), which signals from dendrites in a retrograde manner
533 through presynaptic endocannabinoid receptors to inhibit neurotransmitter release
534 (Hashimotodani et al., 2013; Hashimotodani et al., 2005; Soltesz et al., 2015; Tanimura et al.,
535 2010; Wettschureck et al., 2006). In *C. elegans*, 2-AG activates the NPR-19 endocannabinoid
536 receptor ortholog that couples to $G\alpha_o$ to modulate serotonin transmission, pharyngeal, feeding,
537 and locomotory behaviors (Oakes et al., 2019; Oakes et al., 2017; Pastuhov et al., 2016). We
538 have recently shown that feedback of egg accumulation alters vulval muscle Ca^{2+} activity, which
539 subsequently signals to regulate bursting in the HSNs (Ravi et al., 2018b; Ravi et al., 2020),
540 These results support a model where stretch-dependent feedback of egg accumulation
541 stimulates postsynaptic vulval muscle Ca^{2+} signaling. This Ca^{2+} would then activate PLCs to
542 generate DAG and 2-AG which signal to modulate HSN activity, serotonin release, and egg
543 laying. The genetic and experimental accessibility of the *C. elegans* egg-laying circuit should
544 allow us to determine if conserved G proteins like $G\alpha_q$ act generally to drive neural circuit activity
545 via changes in DAG, subsequent activation of effectors, and retrograde messengers like 2-AG.
546
547

548 **Acknowledgements**

549 This work was funded by grants from the NIH (R01-NS086932) and NSF (IOS-1844657) to KMC.
550 PD is supported by AHA predoctoral fellowship Award (20PRE35210233). We thank Dr. Kenneth
551 Miller for sharing plasmids and strains. Some of the strains used in this study were provided by
552 the *C. elegans* Genetics Center, which is funded by NIH Office of Research Infrastructure
553 Programs (P40 OD010440). We thank Drs. Julia Dallman, Laura Bianchi, and Athula
554 Wikramanayake along with members of the Collins lab for helpful discussions and feedback on
555 the manuscript.

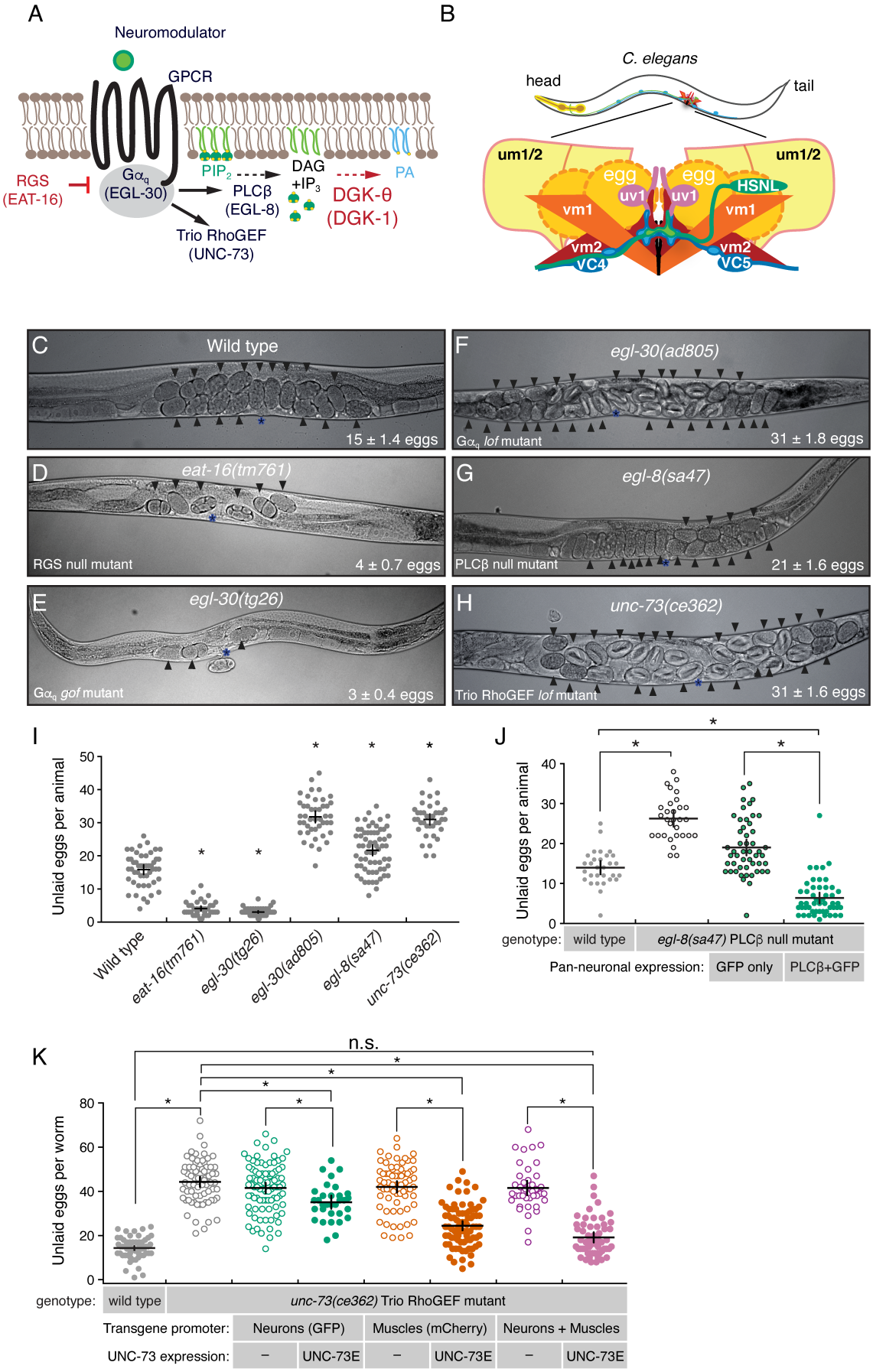
A
Neuromodulator
GPCR
RGS
(EAT-16)
Gαq
(EGL-30)
PIP2
PLCβ
(EGL-8)
DAG
+IP3
DGK-θ
(DGK-1)
PA
Trio RhoGEF
(UNC-73)
B
C. elegans
head
tail
um1/2
um1/2
egg
egg
uv1
uv1
HSNL
vm1
vm1
vm2
vm2
VC4
VC5
C
Wild type
15 ± 1.4 eggs
F
egl-30(ad805)
Gαq lof mutant
31 ± 1.8 eggs
D
eat-16(tm761)
RGS null mutant
4 ± 0.7 eggs
G
egl-8(sa47)
PLCβ null mutant
21 ± 1.6 eggs
E
egl-30(tg26)
Gαq gof mutant
3 ± 0.4 eggs
H
unc-73(ce362)
Trio RhoGEF lof mutant
31 ± 1.6 eggs
I
Unlaid eggs per animal
Wild type
eat-16(tm761)
egl-30(tg26)
egl-30(ad805)
egl-8(sa47)
unc-73(ce362)
J
Unlaid eggs per animal
genotype:
wild type
egl-8(sa47) PLCβ null mutant
Pan-neuronal expression:
GFP only
PLCβ+GFP
K
n.s.
Unlaid eggs per worm
genotype:
wild type
unc-73(ce362) Trio RhoGEF mutant
Transgene promoter:
Neurons (GFP)
Muscles (mCherry)
Neurons + Muscles
UNC-73 expression:
–
UNC-73E
–
UNC-73E
–
UNC-73E

557 **Figure 1: Trio RhoGEF is required in both neurons and muscles to regulate egg-laying**
558 **behavior (A)** Schematics of excitatory (black) and inhibitory (red) $G\alpha_q$ signaling pathway. *C.*
559 *elegans* gene names are beneath the protein they encode. **(B)** Cartoon of the *C. elegans* egg-
560 laying behavior circuit from a lateral view. Only the left side of the bilaterally symmetric circuit is
561 shown. HSNL, Hermaphrodite Specific Neuron (left); VC4 and VC5 Ventral C neurons; vm1 and
562 vm2 vulval muscles, um1 and um2 uterine muscles; uv1 uterine-vulval neuroendocrine cells. **(C-**
563 **H)** Bright field images of worms of the indicated genotypes; arrowheads indicate accumulated
564 eggs. Mean number of accumulated eggs ± 95% confidence intervals is also indicated. Position
565 of the vulva is shown with asterisk (*). **(I)** Scatterplot of egg accumulation in wild-type, *eat-*
566 *16(tm761)*, *egl-30(tg26)*, *egl-30(ad805), egl-8(sa47), and unc-73(ce362)* mutant animals. Line
567 indicates mean eggs ± 95% confidence intervals. Asterisks indicate p ≤0.0001 (One way ANOVA
568 with Bonferroni's correction; wild type n=49; *eat-16(tm761)* n=36; *egl-30(tg26)* n=47; *egl-*
569 *30(ad805)* n=44; *egl-8(sa47)* n=65; *unc-73(ce362)* n=38). **(J)** Transgenic rescue of *egl-8* PLCβ
570 egg-laying defects. Scatterplot of egg accumulation in transgenic animals expressing GFP only
571 or EGL-8/PLCβ fused to GFP from the *rgs-1* promoter in *egl-8(sa47)* null mutants (n=50)
572 compared to wild-type (n=30) and *egl-8(sa47)* mutant animals (n=30). Bar indicates mean eggs
573 ±95% confidence intervals. Asterisks indicate p≤0.0001 (One-way ANOVA with Bonferroni's
574 correction) **(K)** Transgenic rescue of *unc-73* Trio RhoGEF egg-laying defects. Scatterplot of egg
575 accumulation in wild-type (n=60), *unc-73(ce362)* mutants (n=72), and transgenic animals
576 expressing a fluorescent protein with or without Trio in neurons (n≥32) or in muscles (n≥69), or
577 in both neurons and muscles (n≥41) in *unc-73(ce362)* mutants. Horizontal line indicates mean
578 accumulated eggs ±95% confidence intervals. Asterisks indicate p≤0.0145; n.s.= not significant
579 (p>0.05; One-way ANOVA with Bonferroni's correction for multiple comparisons).

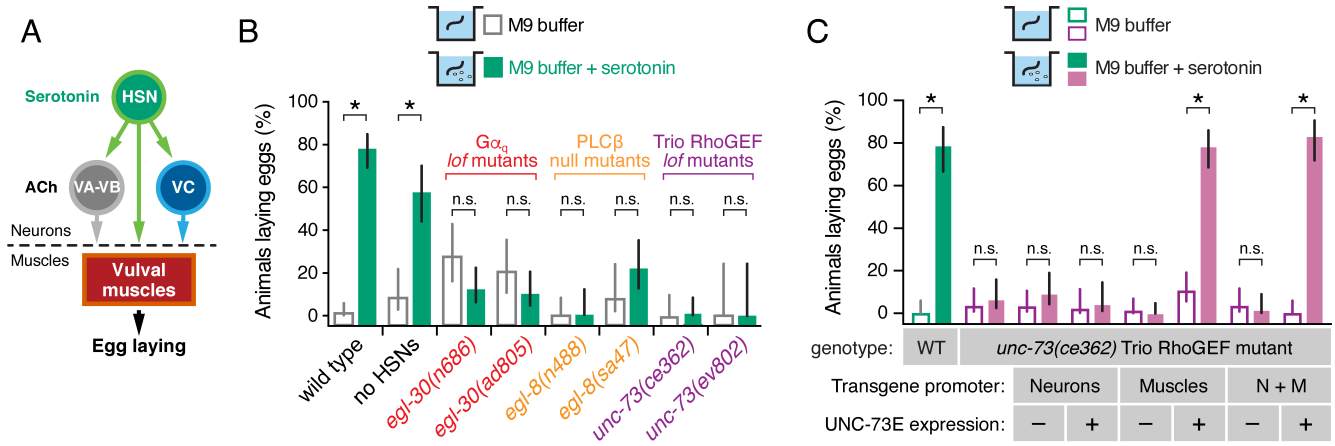

Figure 2: Serotonin signals through $G\alpha_q$, Trio, and PLCβ to promote egg-laying. **(A)** Model of serotonergic and acetylcholine (ACh) signaling in the egg-laying circuit. **(B)** Bar plots showing the percentage of animals laying eggs in M9 buffer alone (grey) or M9 +7.5 mg/mL serotonin (green) in 1 hr. Bar indicates mean percent ±95% confidence intervals. Asterisks indicate p<0.0007; n.s.= not significant (p>0.05, Fisher's exact test with Bonferroni's correction for multiple comparisons; n>30 animals). **(C)** Bar plot showing percent of animals laying eggs in M9 buffer or M9 +7.5 mg/ml serotonin in wild-type or Trio RhoGEF mutant animals expressing nothing or Trio RhoGEF in neurons, muscles, or both. Bar indicates mean percent ±95% confidence intervals. Asterisks indicate p<0.0007; n.s.= not significant (p>0.05, Fisher's exact test with Bonferroni's correction for multiple comparisons; n>30).

591

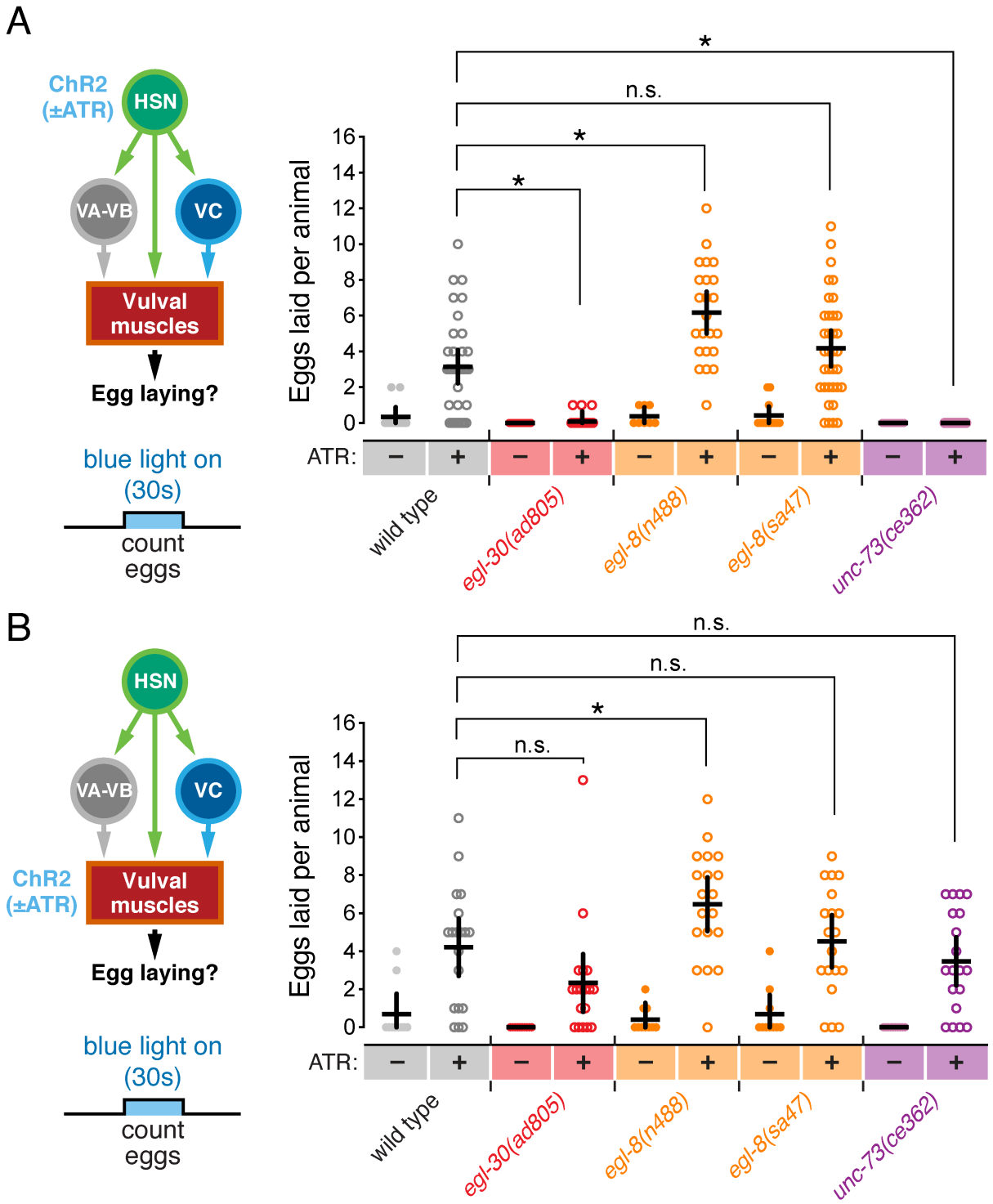

592 **Figure 3: Optogenetic stimulation of the HSNs or vulval muscles indicates cellular**

593 **specificity of Gα_q effectors for egg laying. (A)** On left, cartoon of the egg-laying circuit and

594 experiment showing blue light activation of HSN for 30 seconds. On right, scatterplot showing

595 eggs laid per worm in presence (+) or absence (-) of all-*trans* retinal (ATR) cofactor during the

596 blue light activation of ChR2 expressed in HSNs of wild-type (grey), *egl-30(ad805)* $G\alpha_q$ strong
597 loss-of-function mutants (red), *egl-8(n488) and egl-8(sa47)* PLCβ mutants (orange), and *unc-*
598 *73(ce362)* Trio mutant (purple) animals. Line indicates mean eggs laid ±95% confidence
599 intervals. Asterisks indicate $p<0.0001$; n.s.= not significant ($p>0.05$, One-way ANOVA with
600 Bonferroni's correction for multiple comparisons). (**B)** On the left, cartoon of the egg-laying circuit
601 and experiment showing blue light activation of vulval muscles for 30 seconds(left). On the right,
602 scatter plots of eggs laid per worm in presence (+) or absence (-) of ATR during blue light
603 activation of ChR2 expressed in the vulval muscles of wild type, *egl-30(ad805)* $G\alpha_q$ strong loss-
604 of-function mutants (red), *egl-8(n488) and egl-8(sa47)* PLCβ mutants (orange), and *unc-*
605 *73(ce362)* Trio mutant (purple) animals. Line indicates mean eggs laid ±95% confidence
606 intervals. Asterisk indicates $p\leq0.0255$; n.s.=not significant, $p>0.05$ (One-way ANOVA with
607 Bonferroni's correction for multiple comparisons).

608

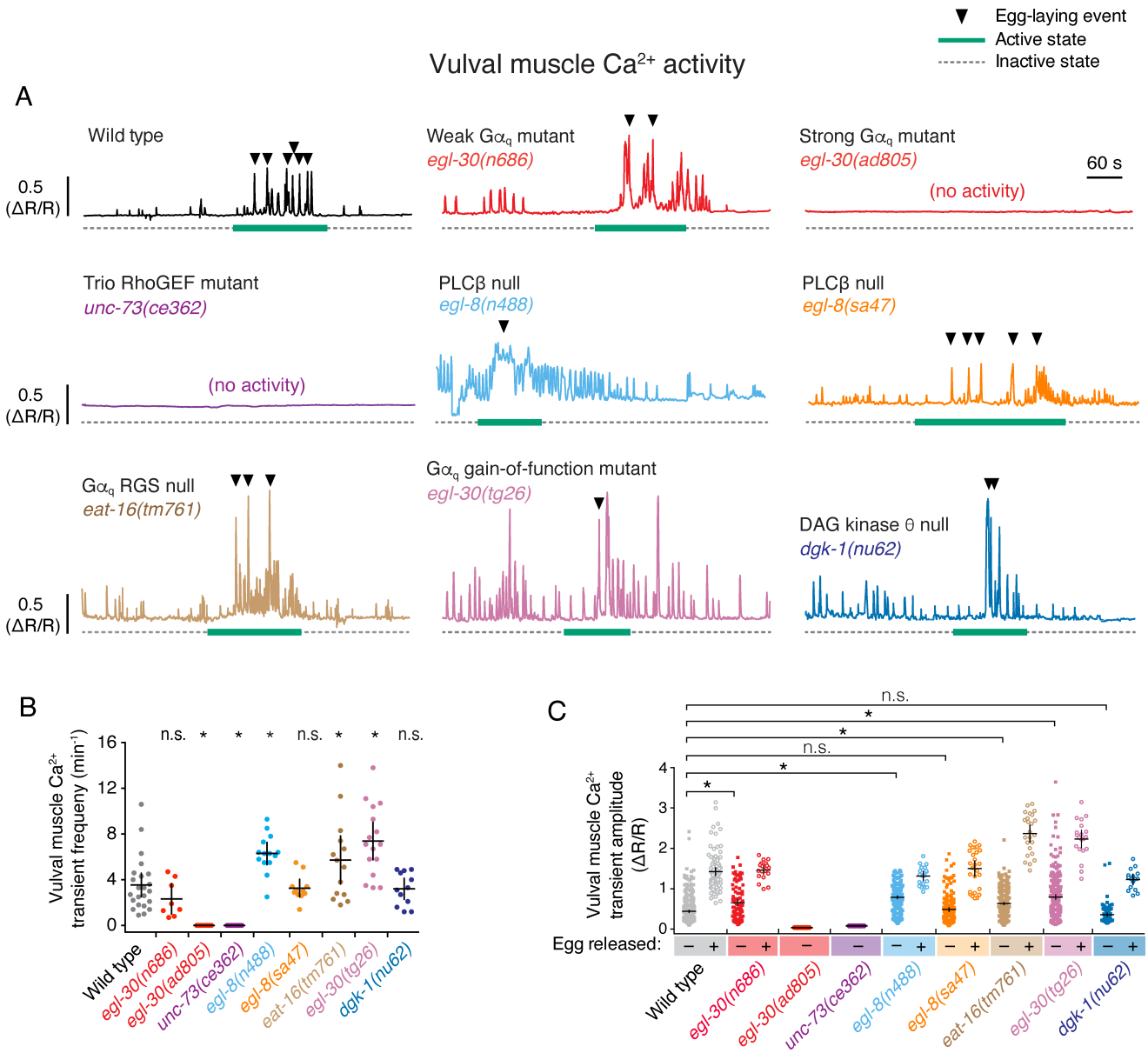

609 **Figure 4: Gα$_q$ and Trio signaling promotes vulval muscle activity. (A)** Representative
610 GCaMP5::mCherry (ΔR/R) ratio traces showing vulval muscle Ca^{2+} activity in freely behaving
611 wild-type (black), *egl-30(n686)* Gα$_q$ weak loss of function mutant (red), *egl-30(ad805)* Gα$_q$
612 strong loss-of-function mutant (red), *unc-73 (ce362)* Trio strong loss-of-function mutant (purple),
613 *egl-8(n488)* PLCβ null mutant (light blue), *egl-8(sa47)* PLCβ null mutant (orange), *eat-16(tm761)*
614 Gα$_q$ RGS protein null mutant (grey), *egl-30(tg26)* strong Gα$_q$ gain-of-function mutant (magenta),
615 and *dgk-1(nu62)* DAG Kinase null mutant (dark blue) animals during active (green solid bar) and

616 inactive (dotted grey line) egg-laying behavior states. Arrowheads indicate egg-laying events;
617 n>10 animals recorded per genotype. **(B)** Scatterplots of Ca^{2+} transient frequency for indicated
618 genotypes. Line indicates mean eggs laid ±95% confidence intervals; asterisks indicate
619 p≤0.0340; n.s. indicates not significant (p>0.05, One-way ANOVA with Bonferroni's correction
620 for multiple comparisons). **(C)** Scatterplots of Ca^{2+} peak amplitudes for the indicated genotypes
621 during twitch (closed square) and egg-laying transients (open circles). Asterisks indicate
622 p<0.0001, n.s. indicates not significant (p>0.05, Kruskal Wallis test with Dunn's correction for
623 multiple comparisons).

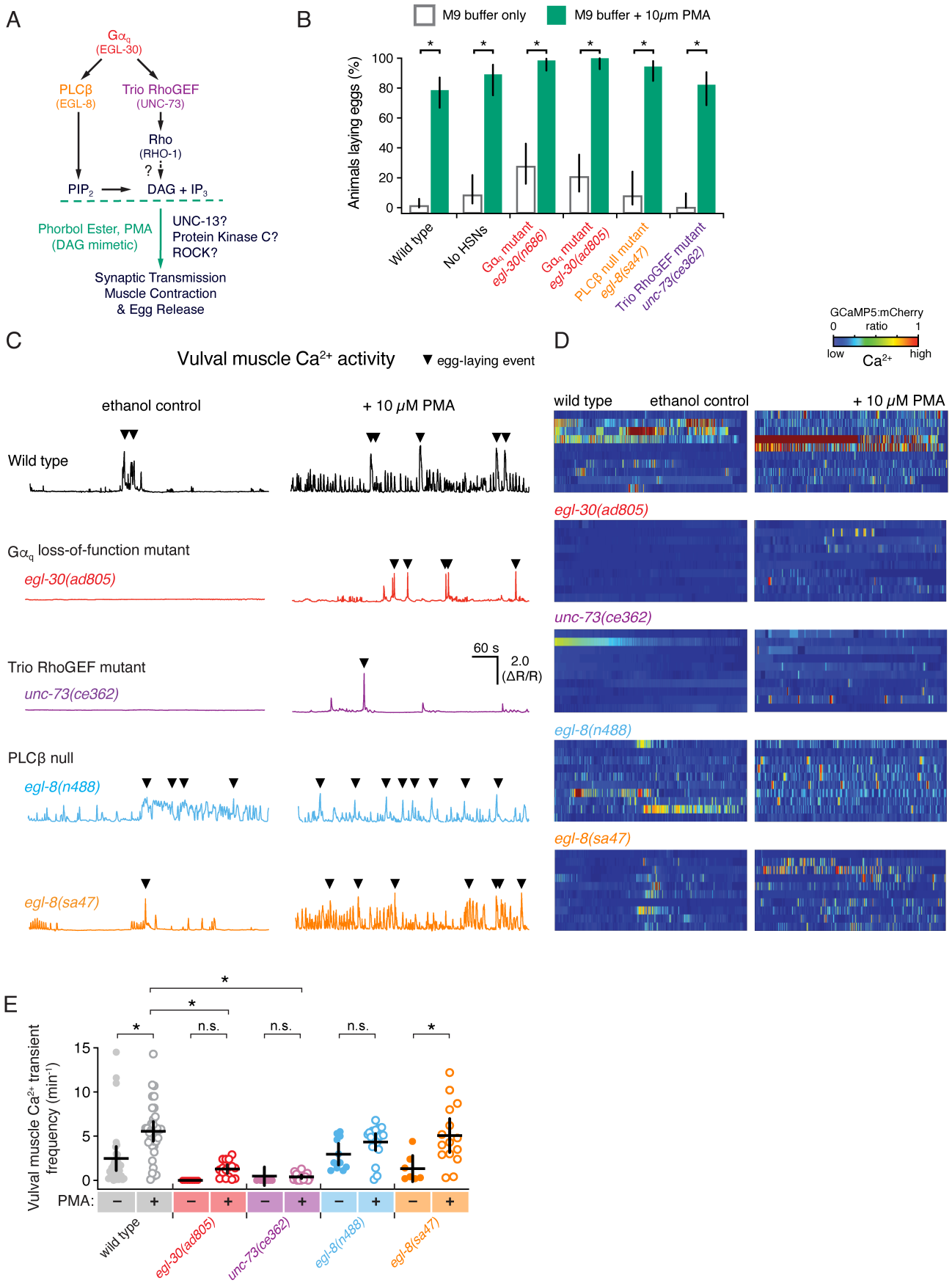
A
Gαq
(EGL-30)
PLCβ
(EGL-8)
Trio RhoGEF
(UNC-73)
Rho
(RHO-1)
?
PIP2
DAG + IP3
Phorbol Ester, PMA
(DAG mimetic)
UNC-13?
Protein Kinase C?
ROCK?
Synaptic Transmission
Muscle Contraction
& Egg Release
B
M9 buffer only
M9 buffer + 10μm PMA
Animals laying eggs (%)
100
80
60
40
20
0
Wild type
No HSNs
Gαq mutant
egl-30(n686)
Gαq mutant
egl-30(ad805)
PLCβ null mutant
egl-8(sa47)
Trio RhoGEF mutant
unc-73(ce362)
C
Vulval muscle Ca2+ activity
▼ egg-laying event
ethanol control
+ 10 μM PMA
Wild type
Gαq loss-of-function mutant
egl-30(ad805)
Trio RhoGEF mutant
unc-73(ce362)
60 s
2.0
(ΔR/R)
PLCβ null
egl-8(n488)
egl-8(sa47)
D
GCaMP5:mCherry
0
ratio
1
low
Ca2+
high
wild type
ethanol control
+ 10 μM PMA
egl-30(ad805)
unc-73(ce362)
egl-8(n488)
egl-8(sa47)
E
Vulval muscle Ca2+ transient
frequency (min-1)
15
10
5
0
PMA:
−
+
n.s.
wild type
egl-30(ad805)
unc-73(ce362)
egl-8(n488)
egl-8(sa47)

625 **Figure 5: DAG mimetic PMA rescues egg-laying circuit activity and behavior defects of**
626 **Gα_q signaling mutants**. **(A)** Diagrams showing working model of Gα_q and DAG signaling
627 pathway during egg-laying behavior. **(B)** Bar plots showing the percentage of animals showing
628 egg laying in M9 buffer (open grey bars) or M9 buffer +10 μM PMA (filled green bars). Error bars
629 indicate 95% confidence intervals for the proportion. Asterisks indicate $p<0.0006$ (Fisher's exact
630 test with Bonferroni's correction for multiple comparisons). **(C)** Representative
631 GCaMP5::mCherry (ΔR/R) ratio traces showing vulval muscle Ca^{2+} activity in wild-type or the
632 indicated Gα_q signaling mutant animals in the absence (left) or presence (right) of 10 μM PMA.
633 Arrowheads indicate egg-laying events. Number of animals recorded for each genotype and
634 condition, n>10. **(D)** Heat map showing intensity modulated color spectrum of
635 GCaMP5::mCherry (ΔR/R) ratio of vulval muscle Ca^{2+} activity ranging from blue (low Ca^{2+}) to
636 red (high Ca^{2+}) of 10 animals. **(E)** Scatterplots of Ca^{2+} transient frequency in the absence (-) and
637 presence (+) of 10 μM PMA for the indicated genotypes. Line indicates mean eggs laid ±95%
638 confidence intervals. Asterisk indicates $p\leq0.0275$; n.s.= not significant ($p>0.05$, One-way
639 ANOVA with Bonferroni's correction for multiple comparisons).
640

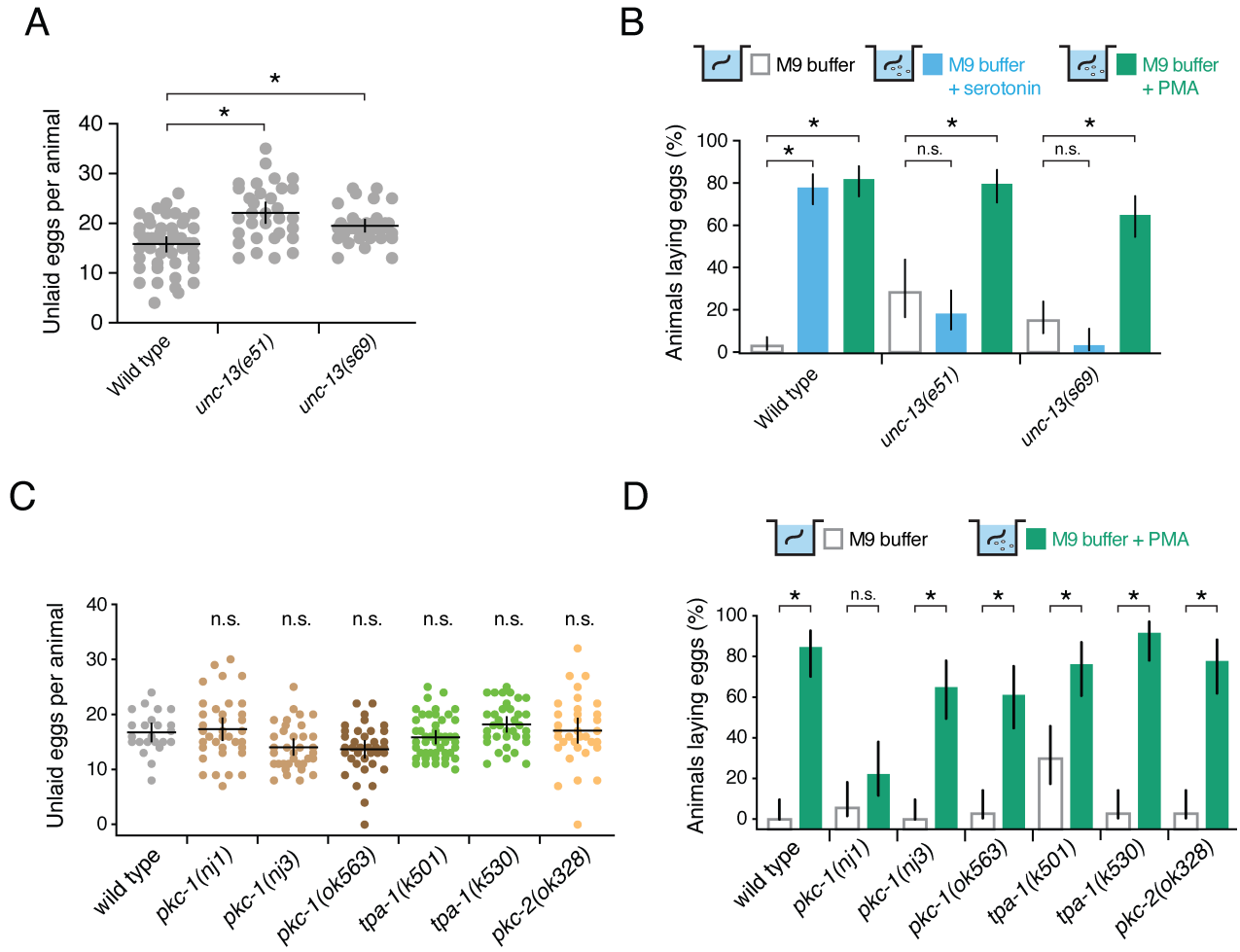

Figure 6: DAG promotes egg laying independent of UNC-13 or Protein Kinase C. (A) Scatterplot of egg accumulation in wild-type, *unc-13(e51)* loss-of-function mutant, and *unc-13(s69)* null mutant animals. Line indicates mean eggs laid ±95% confidence intervals. Asterisk indicates p ≤0.0021 (One-way ANOVA with Bonferroni's correction for multiple comparisons). (**B)** Bar plots showing the percentage of wild-type, *unc-13(e51),* or *unc-13(s69)* mutant animals laying eggs in M9 buffer (grey open boxes), 7.5 mg/ml serotonin (filled blue boxes), or 10 μM PMA (filled green boxes). Bar indicates mean eggs ±95% confidence interval for the proportion. Asterisks indicate p<0.0006; n. s = not significant (p>0.05, Fisher's exact test with Bonferroni's correction for multiple comparisons). **(C)** Scatterplot of egg accumulation in wild-type and indicated Protein Kinase C mutant animals. Line indicates average eggs accumulated ±95% confidence intervals. n.s.= not significant (p>0.05, One-way ANOVA with Bonferroni's correction

653 for multiple comparisons). **(D)** Bar plots showing the percentage of wild-type and Protein Kinase
654 C mutant animals showing egg laying in M9 buffer (open bars) or 10 μM PMA (filled green bars).
655 Bar indicates mean eggs ±95% confidence intervals for the proportion. Asterisks indicate
656 $p<0.0007$; n.s.= not significant ($p>0.05$, Fisher's exact test with Bonferroni correction for multiple
657 comparisons).
658

659 **Movie 1: GCaMP5:mCherry fluorescence ratio in the vulval muscles of wild-type animals**
660 **in the absence or presence of 10 μM DAG analogue, PMA.** Blue indicates low Ca^{2+}, and red
661 indicates elevated Ca^{2+}.
662
663 **Movie 2: GCaMP5:mCherry fluorescence ratio in the vulval muscles of strong loss of**
664 **function $G\alpha_q$ mutant, *egl-30(ad805),* in the absence or presence of 10 μM DAG analogue,**
665 **PMA.** Blue indicates low Ca^{2+}, and red indicates elevated Ca^{2+}.
666
667 **Movie 3: GCaMP5:mCherry fluorescence ratio in the vulval muscles of strong loss of**
668 **function Trio mutant, *unc-73(ce362)*, animals in the absence or presence of PMA.** Blue
669 indicates low Ca^{2+}, and red indicates elevated Ca^{2}.
670
671 **Table 1: Lists of *C. elegans* strains used in this study**
672

Strains	Genotype	Feature	Figure(s)	Source
N2	Wild type	Bristol wild-type strain	1,2,5	(Brenner, 1974)
MT1434	*egl-30(n686) I*	$G\alpha_q$ loss-of-function mutant, Egg-laying defective	1,2,5	(Trent et al., 1983)
DA823	*egl-30(ad805) I*	$G\alpha_q$ strong loss-of-function mutant, Egg-laying defective	1,2,5	(Brundage et al., 1996; Mendel et al., 1995)
KG1278	*unc-73(ce362) I*	Trio RhoGEF loss-of-function mutant, Egg-laying defective	1,2	(Williams et al., 2007)

KG1397	*unc-73(ev802) I*	Trio RhoGEF deletion mutant, Egg-laying defective	2,5	(Williams et al., 2007)
JT47	*egl-8(sa47) V*	PLCβ null, Egg-laying defective	1,2,5	(Thomas, 1990)
MT1083	*egl-8(n488) V*	PLCβ null, Egg-laying defective	2	(Trent et al., 1983)
LX1226	*eat-16(tm761) I*	$G\alpha_q$ RGS null, Hyperactive egg laying	1	(Porter and Koelle, 2010)
CG21	*egl-30(tg26) I; him-5(e1490) V*	$G\alpha_q$ gain-of-function mutant, Hyperactive egg-laying	1	(Garcia et al., 2001)
LX1832	*lite-1(ce314) lin-15(n765ts) X*	strain used for transgenic line creation		(Gürel et al., 2012)
LX1286	*egl-8(sa47) I; lin-15(n765ts) X*	PLCβ null mutant, Egg-laying defective; multi-vulva	1	This study
LX1674	*egl-8(sa47) I; lin-15(n765ts) X; vsEx679*	PLCβ null, Egg-laying defective; non-Muv, expresses GFP in neurons from *rgs-1* promoter	1	This study
LX1675	*egl-8(sa47) I; lin-15(n765ts) X; vsEx680*	PLCβ null, Egg laying defective; non-Muv, expresses PLCβ and GFP in neurons from *rgs-1* promoter	1	This study
MIA26	*egl-1(n986dm) V*	Lacks HSNs	2,5	(Ravi et al., 2018a)
LX1918	*vsIs164 lite-1(ce314) lin-15(n765ts) X*	Expresses GCaMP5 and mCherry in the vulval muscles	4,5	(Li et al., 2013)

MIA109	*egl-8(sa47) V; vsIs164 lite-1(ce314), lin-15(n765ts) X*	Expresses GCaMP5 and mCherry in the vulval muscles of *egl-8(sa47)* mutant	4,5	This study
MIA139	*egl-30(n686) I; vsIs164 lite-1(ce314) lin-15(n765ts) X*	Expresses GCaMP5 and mCherry in the vulval muscles of *egl-30(n686*)	4,5	This study
MIA140	*egl-30(ad805) I; vsIs164 lite-1(ce314), lin-15(n765ts) X*	Expresses GCaMP5 and mCherry in the vulval muscles of *egl-30(ad805)*	4,5	This study
MIA141	*unc-73(ce362) I; vsIs164, lite-1(ce314) lin-15(n765ts) X*	Expresses GCaMP5 and mCherry in the vulval muscles of *unc-73(ce362)*	4,5	This study
MIA286	*egl-30(tg26) I; vsIs164, lite-1(ce314) lin-15(n765ts) X*	Expresses GCaMP5 and mCherry in the vulval muscles of *egl-30(tg26)*	4	This study
MIA287	*eat-16(tm761) I; vsIs164 lite-1(ce314) lin-15(n765ts) X*	Expresses GCaMP5 and mCherry in the vulval muscles of *eat-16(tm761)*	4	This study

MIA288	*egl-8(n488) V; vsIs164 lite-1 (ce314) lin-15(n765ts) X*	Expresses GCaMP5 and mCherry in the vulval muscles of *egl-8(n488)*	4,5	This study
MIA296	*dgk-1(nu62) lite-1(ce314) lin-15(n765ts) X*	Expresses GCaMP5 and mCherry in the vulval muscles of *dgk-1(nu62)*	4	This study
MIA372	*unc-73(ce362) I; keyEx64*	Expresses GFP in the neurons and mCherry in the muscles of *unc-73(ce362)*	1	This study
MIA373	*unc-73(ce362) I; keyEx65*	Expresses GFP and Trio RhoGEF-E cDNA in the neurons, and mCherry and Trio RhoGEF-E cDNA in the muscles of *unc-73(ce362)*	1	This study
MIA374	*unc-73(ce362) I; keyEx66*	Expresses GFP in neurons	1	This study
MIA375	*unc-73(ce362) I; keyEx67*	Expresses GFP and Trio RhoGEF-E cDNA in neurons	1	This study
MIA376	*unc-73(ce362) I; keyEx68*	Expresses mCherry in muscles	1,2	This study
MIA377	*unc-73(ce362) I; keyEx69*	Expresses mCherry and Trio RhoGEF-E cDNA in muscles	1,2	This study

LX1836	*wzIs30 IV; lite-1(ce314) lin-15(n765ts) X*	Expresses Channelrhodopsin-2 (ChR2) in HSNs from the *egl-6* promoter	3	(Collins et al., 2016)
MIA229	*keyIs48; lite-1(ce314) lin-15(n765ts) X*	Expresses ChR2 in vulval muscles from the *ceh-24* promoter	3	(Kopchock et al., 2020)
MIA300	*egl-30(ad805) I; wzIs30 IV; lite-1(ce314) X*	Expresses ChR2 in HSN of *egl-30(ad805)* mutant	3	This study
MIA301	*egl-30(ad805) I; keyIs48; lite-1(ce314) X*	Expresses ChR2 in vulval muscles of *egl-30(ad805)* mutant	3	This study
MIA304	*wzIs30 IV; egl-8(n488) V; lite-1(ce314) X*	Expresses ChR2 in HSNs of *egl-8(n488)* mutant	3	This study
MIA305	*egl-8(n488) V; keyIs48; lite-1(ce314) X*	Expresses ChR2 in vulval muscles of *egl-8(n488)* mutant	3	This study
MIA308	*wzIs30 IV; egl-8(sa47) V; lite-1(ce314) X*	Express ChR2 in HSNs of *egl-8(sa47)* mutant	3	This study
MIA309	*egl-8(sa47) V; keyIs48; lite-1(ce314) X*	Expresses ChR2 in vulval muscles of *egl-8(sa47)* mutant	3	This study

MIA247	*unc-73(ce362) I; wzIs30 IV; lite-1(ce314) X*	Expresses ChR2 in HSN of *unc-73(ce362)* mutant	3	This study
MIA248	*unc-73(ce362) I; keyIs48; lite-1(ce314) X*	Expresses ChR2 in vulval muscles of *unc-73(ce362)* mutant	3	This study
MT7929	*unc-13(e51) I*	UNC-13 loss-of-function	6	(Brenner, 1974)
EG9631	*unc-13(s69) I*	UNC-13 null	6	(Rose and Baillie, 1980)
IK105	*pkc-1(nj1) V*	nPKCε null	6	(Okochi et al., 2005)
IK130	*pkc-1(nj3) V*	nPKCε null	6	(Okochi et al., 2005)
RB781	*pkc-1(ok563) V*	nPKCε null	6	(Consortium, 2012)
VC127	*pkc-2(ok328) X*	cPKCα/β null	6	(Consortium, 2012)
MJ500	*tpa-1(k501) IV*	nPKCδ/θ null	6	(Tabuse et al., 1989)
MJ563	*tpa-1(k530) IV*	nPKCδ/θ null	6	(Tabuse et al., 1989)

673

674

675 **Table 2: Lists of oligonucleotide sequences used in this study**

Oligo Name	Sequence (5'>3')	Use
lite-1(ce314)-fwd	ACGGGAGACGAAGAGCTAAATAGG	Genotyping of *lite-1(ce314)*
lite-1(ce314)-rev	CTAAGTTGCCGGTTGCCTTAGAAC	Genotyping of *lite-1(ce314)*
egl-30(n686)-F	GCCAACCGAGCAGGACATTCTGCG	Genotyping of *egl-30(n686)*
eg-30(n686)-R	CGGGAAAGTAGTCAGCGAGATGCG	Genotyping of *egl-30(n686)*
egl-30(ad805)-F	GCCAGGGCTGTCCCATTACGG	Genotyping of *egl-30(ad805)*
egl-30(ad805)-R	TCGGAAAGCGCCACCAGGAAC	Genotyping of *egl-30(ad805)*
egl-8-cDNA-fwd	CTTGGCTAGCGTAGAAAAAATGGCAAAGGAGTTCCAGTTC	For amplification of *egl-8* coding sequences
egl-8-cDNA-rev	CGCCCATGGTTATCAAACGACAGAAGTCGGTTGAGC	For amplification of *egl-8* coding sequences
egl-8-Cterm-NotI-fwd	GTGGGTACTCCACTGGGGGTGCGGCCGCTGGAGGTCCTTCGACACCGGT	Quick change mutagenesis of *egl-8* cDNA to insert in-frame NotI enzyme for GFP insertion
egl-8-Cterm-NotI-rev	ACCGGTGTCGAAGGACCTCCAGCGGCCGCACCCCCAGTGGAGTACCCAC	Quick-change mutagenesis of *egl-8* cDNA to insert in-frame NotI enzyme for GFP insertion

NotI-GFP-FWD	GGTGCGGCCGCTGGAAGTAAA GGAGAAGAACTTTTC	For amplification of GFP with flanking, in-frame NotI enzyme sites for insertion into *egl-8* cDNA
NotI-GFP-REV	TCCAGCGGCCGCTCCTTTGTAT AGTTCATCCATGCC	For amplification of GFP with flanking, in-frame NotI enzyme sites for insertion into *egl-8* cDNA
RE-GFP-FWD-new	GCGTCTAGAACCGGTGCTAGC GTAGAAAAAATGGTCAGTAAAG GAGAAGAACTTTTC	For amplification of sequences encoding GFP for cloning into pGP3 *rgs-1* promoter containing plasmid
RE-GFP-REV	TACGAATTCGGTACCTCAGATT TATTTGTATAGTTCATCCATG	For amplification of sequences encoding GFP for cloning into pGP3 *rgs-1* promoter containing plasmid

676

677 **References:**

678 Akerboom, J., Carreras Calderon, N., Tian, L., Wabnig, S., Prigge, M., Tolo, J., Gordus, A., Orger, M.B.,
679 Severi, K.E., Macklin, J.J.*, et al.* (2013). Genetically encoded calcium indicators for multi-
680 color neural activity imaging and combination with optogenetics. Front Mol Neurosci *6*, 2.

681 Ananthanarayanan, B., Stahelin, R.V., Digman, M.A., and Cho, W. (2003). Activation mechanisms of
682 conventional protein kinase C isoforms are determined by the ligand affinity and
683 conformational flexibility of their C1 domains. J Biol Chem *278*, 46886-46894.

684 Avery, L., Bargmann, C.I., and Horvitz, H.R. (1993). The Caenorhabditis elegans unc-31 gene affects
685 multiple nervous system-controlled functions. Genetics *134*, 455-464.

686 Banerjee, N., Bhattacharya, R., Gorczyca, M., Collins, K.M., and Francis, M.M. (2017). Local
687 neuropeptide signaling modulates serotonergic transmission to shape the temporal
688 organization of C. elegans egg-laying behavior. PLoS Genet *13*, e1006697.

689 Bastiani, C.A., Gharib, S., Simon, M.I., and Sternberg, P.W. (2003). Caenorhabditis elegans Galphaq
690 regulates egg-laying behavior via a PLCbeta-independent and serotonin-dependent
691 signaling pathway and likely functions both in the nervous system and in muscle. Genetics
692 *165*, 1805-1822.

693 Berridge, M.J., Lipp, P., and Bootman, M.D. (2000). The versatility and universality of calcium signalling.
694 Nat Rev Mol Cell Biol *1*, 11-21.

695 Betke, K.M., Wells, C.A., and Hamm, H.E. (2012). GPCR mediated regulation of synaptic transmission.
696 Prog Neurobiol *96*, 304-321.

697 Betz, A., Ashery, U., Rickmann, M., Augustin, I., Neher, E., Sudhof, T.C., Rettig, J., and Brose, N. (1998).
698 Munc13-1 is a presynaptic phorbol ester receptor that enhances neurotransmitter release.
699 Neuron *21*, 123-136.

700 Brenner, S. (1974). The genetics of Caenorhabditis elegans. Genetics *77*, 71-94.

701 Brewer, J.C., Olson, A.C., Collins, K.M., and Koelle, M.R. (2019). Serotonin and neuropeptides are both
702 released by the HSN command neuron to initiate Caenorhabditis elegans egg laying. PLoS
703 Genet *15*, e1007896.

704 Brose, N., and Rosenmund, C. (2002). Move over protein kinase C, you've got company: alternative
705 cellular effectors of diacylglycerol and phorbol esters. J Cell Sci *115*, 4399-4411.

706 Brundage, L., Avery, L., Katz, A., Kim, U.J., Mendel, J.E., Sternberg, P.W., and Simon, M.I. (1996).
707 Mutations in a C. elegans Gqalpha gene disrupt movement, egg laying, and viability. Neuron
708 *16*, 999-1009.

709 Chang, Y.C., Lee, H.H., Chen, Y.J., Bokoch, G.M., and Chang, Z.F. (2006). Contribution of guanine
710 exchange factor H1 in phorbol ester-induced apoptosis. Cell Death Differ *13*, 2023-2032.

711 Chase, D.L., Pepper, J.S., and Koelle, M.R. (2004). Mechanism of extrasynaptic dopamine signaling in
712 Caenorhabditis elegans. Nat Neurosci *7*, 1096-1103.

713 Chhatriwala, M.K., Betts, L., Worthylake, D.K., and Sondek, J. (2007). The DH and PH domains of Trio
714 coordinately engage Rho GTPases for their efficient activation. J Mol Biol *368*, 1307-1320.

715 Coleman, B., Topalidou, I., and Ailion, M. (2018). Modulation of Gq-Rho Signaling by the ERK MAPK
716 Pathway Controls Locomotion in Caenorhabditis elegans. Genetics *209*, 523-535.

717 Collins, K.M., Bode, A., Fernandez, R.W., Tanis, J.E., Brewer, J.C., Creamer, M.S., and Koelle, M.R.
718 (2016). Activity of the C. elegans egg-laying behavior circuit is controlled by competing
719 activation and feedback inhibition. Elife *5*.

720 Collins, K.M., and Koelle, M.R. (2013). Postsynaptic ERG potassium channels limit muscle excitability to
721 allow distinct egg-laying behavior states in Caenorhabditis elegans. J Neurosci *33*, 761-775.

722 Consortium, C.e.D.M. (2012). large-scale screening for targeted knockouts in the Caenorhabditis
723 elegans genome. G3 (Bethesda) *2*, 1415-1425.
724 Cook, S.J., Jarrell, T.A., Brittin, C.A., Wang, Y., Bloniarz, A.E., Yakovlev, M.A., Nguyen, K.C.Q., Tang, L.T.,
725 Bayer, E.A., Duerr, J.S.*, et al.* (2019). Whole-animal connectomes of both Caenorhabditis
726 elegans sexes. Nature *571*, 63-71.
727 Dempsey, C.M., Mackenzie, S.M., Gargus, A., Blanco, G., and Sze, J.Y. (2005). Serotonin (5HT),
728 fluoxetine, imipramine and dopamine target distinct 5HT receptor signaling to modulate
729 Caenorhabditis elegans egg-laying behavior. Genetics *169*, 1425-1436.
730 Doi, M., and Iwasaki, K. (2002). Regulation of retrograde signaling at neuromuscular junctions by the
731 novel C2 domain protein AEX-1. Neuron *33*, 249-259.
732 Dong, M.Q., Chase, D., Patikoglou, G.A., and Koelle, M.R. (2000). Multiple RGS proteins alter neural G
733 protein signaling to allow C. elegans to rapidly change behavior when fed. Genes Dev *14*,
734 2003-2014.
735 Edwards, M.R., Johnson, J.R., Rankin, K., Jenkins, R.E., Maguire, C., Morgan, A., Burgoyne, R.D., and
736 Barclay, J.W. (2012). PKC-2 phosphorylation of UNC-18 Ser322 in AFD neurons regulates
737 temperature dependency of locomotion. J Neurosci *32*, 7042-7051.
738 Emtage, L., Aziz-Zaman, S., Padovan-Merhar, O., Horvitz, H.R., Fang-Yen, C., and Ringstad, N. (2012).
739 IRK-1 potassium channels mediate peptidergic inhibition of Caenorhabditis elegans
740 serotonin neurons via a G(o) signaling pathway. J Neurosci *32*, 16285-16295.
741 Fernandez, R.W., Wei, K., Wang, E.Y., Mikalauskaite, D., Olson, A., Pepper, J., Christie, N., Kim, S.,
742 Weissenborn, S., Sarov, M.*, et al.* (2020). Cellular Expression and Functional Roles of All 26
743 Neurotransmitter GPCRs in the C. elegans Egg-Laying Circuit. J Neurosci *40*, 7475-7488.

744 Garcia, L.R., Mehta, P., and Sternberg, P.W. (2001). Regulation of distinct muscle behaviors controls the
745 C. elegans male's copulatory spicules during mating. Cell *107*, 777-788.
746 Geppetti, P., Veldhuis, N.A., Lieu, T., and Bunnett, N.W. (2015). G Protein-Coupled Receptors: Dynamic
747 Machines for Signaling Pain and Itch. Neuron *88*, 635-649.
748 Gürel, G., Gustafson, M.A., Pepper, J.S., Horvitz, H.R., and Koelle, M.R. (2012). Receptors and other
749 signaling proteins required for serotonin control of locomotion in Caenorhabditis elegans.
750 Genetics *192*, 1359-1371.
751 Hajdu-Cronin, Y.M., Chen, W.J., Patikoglou, G., Koelle, M.R., and Sternberg, P.W. (1999). Antagonism
752 between G(o)alpha and G(q)alpha in Caenorhabditis elegans: the RGS protein EAT-16 is
753 necessary for G(o)alpha signaling and regulates G(q)alpha activity. Genes Dev *13*, 1780-
754 1793.
755 Hashimotodani, Y., Ohno-Shosaku, T., and Kano, M. (2006). [Mechanisms of triggering
756 endocannabinoid release]. Seikagaku *78*, 126-130.
757 Hashimotodani, Y., Ohno-Shosaku, T., Tanimura, A., Kita, Y., Sano, Y., Shimizu, T., Di Marzo, V., and
758 Kano, M. (2013). Acute inhibition of diacylglycerol lipase blocks endocannabinoid-mediated
759 retrograde signalling: evidence for on-demand biosynthesis of 2-arachidonoylglycerol. J
760 Physiol *591*, 4765-4776.
761 Hashimotodani, Y., Ohno-Shosaku, T., Tsubokawa, H., Ogata, H., Emoto, K., Maejima, T., Araishi, K.,
762 Shin, H.S., and Kano, M. (2005). Phospholipase Cbeta serves as a coincidence detector
763 through its Ca2+ dependency for triggering retrograde endocannabinoid signal. Neuron *45*,
764 257-268.

765 Hashimotodani, Y., Ohno-Shosaku, T., Watanabe, M., and Kano, M. (2007). Roles of phospholipase
766 Cbeta and NMDA receptor in activity-dependent endocannabinoid release. J Physiol *584*,
767 373-380.
768 Hiley, E., McMullan, R., and Nurrish, S.J. (2006). The Galpha12-RGS RhoGEF-RhoA signalling pathway
769 regulates neurotransmitter release in C. elegans. Embo j *25*, 5884-5895.
770 Hoyt, J.M., Wilson, S.K., Kasa, M., Rise, J.S., Topalidou, I., and Ailion, M. (2017). The SEK-1 p38 MAP
771 Kinase Pathway Modulates Gq Signaling in Caenorhabditis elegans. G3 (Bethesda) *7*, 2979-
772 2989.
773 Hu, S., Pawson, T., and Steven, R.M. (2011). UNC-73/trio RhoGEF-2 activity modulates Caenorhabditis
774 elegans motility through changes in neurotransmitter signaling upstream of the GSA-
775 1/Galphas pathway. Genetics *189*, 137-151.
776 Huang, K.P. (1989). The mechanism of protein kinase C activation. Trends Neurosci *12*, 425-432.
777 Hyde, R., Corkins, M.E., Somers, G.A., and Hart, A.C. (2011). PKC-1 acts with the ERK MAPK signaling
778 pathway to regulate Caenorhabditis elegans mechanosensory response. Genes Brain Behav
779 *10*, 286-298.
780 Jacob, T.C., and Kaplan, J.M. (2003). The EGL-21 carboxypeptidase E facilitates acetylcholine release at
781 Caenorhabditis elegans neuromuscular junctions. J Neurosci *23*, 2122-2130.
782 Jantsch-Plunger, V., Gönczy, P., Romano, A., Schnabel, H., Hamill, D., Schnabel, R., Hyman, A.A., and
783 Glotzer, M. (2000). CYK-4: A Rho family gtpase activating protein (GAP) required for central
784 spindle formation and cytokinesis. J Cell Biol *149*, 1391-1404.
785 Jose, A.M., and Koelle, M.R. (2005). Domains, amino acid residues, and new isoforms of Caenorhabditis
786 elegans diacylglycerol kinase 1 (DGK-1) important for terminating diacylglycerol signaling in
787 vivo. J Biol Chem *280*, 2730-2736.

788 Kass, J., Jacob, T.C., Kim, P., and Kaplan, J.M. (2001). The EGL-3 proprotein convertase regulates
789 mechanosensory responses of Caenorhabditis elegans. J Neurosci *21*, 9265-9272.
790 Kim, J., Poole, D.S., Waggoner, L.E., Kempf, A., Ramirez, D.S., Treschow, P.A., and Schafer, W.R. (2001).
791 Genes affecting the activity of nicotinic receptors involved in Caenorhabditis elegans egg-
792 laying behavior. Genetics *157*, 1599-1610.
793 Konig, B., DiNitto, P.A., and Blumberg, P.M. (1985). Stoichiometric binding of diacylglycerol to the
794 phorbol ester receptor. J Cell Biochem *29*, 37-44.
795 Kopchock, R.J., 3rd, Ravi, B., Bode, A., and Collins, K.M. (2021). The sex-specific VC neurons are
796 mechanically activated motor neurons that facilitate serotonin-induced egg laying in C.
797 elegans. J Neurosci.
798 Kopchock, R.J., Ravi, B., Bode, A., and Collins, K.M. (2020). The female-specific VC neurons are
799 mechanically activated, feed-forward motor neurons that facilitate serotonin-induced egg
800 laying in C. elegans. bioRxiv, 2020.2008.2011.246942.
801 Kunitomo, H., Sato, H., Iwata, R., Satoh, Y., Ohno, H., Yamada, K., and Iino, Y. (2013). Concentration
802 memory-dependent synaptic plasticity of a taste circuit regulates salt concentration
803 chemotaxis in Caenorhabditis elegans. Nat Commun *4*, 2210.
804 Lackner, M.R., Nurrish, S.J., and Kaplan, J.M. (1999). Facilitation of synaptic transmission by EGL-30
805 Gqalpha and EGL-8 PLCbeta: DAG binding to UNC-13 is required to stimulate acetylcholine
806 release. Neuron *24*, 335-346.
807 Li, B., Jie, W., Huang, L., Wei, P., Li, S., Luo, Z., Friedman, A.K., Meredith, A.L., Han, M.H., Zhu, X.H.*, et al.*
808 (2014). Nuclear BK channels regulate gene expression via the control of nuclear calcium
809 signaling. Nat Neurosci *17*, 1055-1063.

810 Li, P., Collins, K.M., Koelle, M.R., and Shen, K. (2013). LIN-12/Notch signaling instructs postsynaptic
811 muscle arm development by regulating UNC-40/DCC and MADD-2 in Caenorhabditis
812 elegans. Elife *2*, e00378.
813 Lou, X., Korogod, N., Brose, N., and Schneggenburger, R. (2008). Phorbol esters modulate spontaneous
814 and Ca2+-evoked transmitter release via acting on both Munc13 and protein kinase C. J
815 Neurosci *28*, 8257-8267.
816 Lutz, S., Freichel-Blomquist, A., Yang, Y., Rumenapp, U., Jakobs, K.H., Schmidt, M., and Wieland, T.
817 (2005). The guanine nucleotide exchange factor p63RhoGEF, a specific link between Gq/11-
818 coupled receptor signaling and RhoA. J Biol Chem *280*, 11134-11139.
819 Maruyama, I.N., and Brenner, S. (1991). A phorbol ester/diacylglycerol-binding protein encoded by the
820 unc-13 gene of Caenorhabditis elegans. Proc Natl Acad Sci U S A *88*, 5729-5733.
821 McMullan, R., Hiley, E., Morrison, P., and Nurrish, S.J. (2006). Rho is a presynaptic activator of
822 neurotransmitter release at pre-existing synapses in C. elegans. Genes Dev *20*, 65-76.
823 McMullan, R., and Nurrish, S.J. (2011). The RHO-1 RhoGTPase modulates fertility and multiple
824 behaviors in adult C. elegans. PLoS One *6*, e17265.
825 Mendel, J.E., Korswagen, H.C., Liu, K.S., Hajdu-Cronin, Y.M., Simon, M.I., Plasterk, R.H., and Sternberg,
826 P.W. (1995). Participation of the protein Go in multiple aspects of behavior in C. elegans.
827 Science *267*, 1652-1655.
828 Miller, K.G., Alfonso, A., Nguyen, M., Crowell, J.A., Johnson, C.D., and Rand, J.B. (1996). A genetic
829 selection for Caenorhabditis elegans synaptic transmission mutants. Proc Natl Acad Sci U S A
830 *93*, 12593-12598.
831 Miller, K.G., Emerson, M.D., and Rand, J.B. (1999). Goalpha and diacylglycerol kinase negatively
832 regulate the Gqalpha pathway in C. elegans. Neuron *24*, 323-333.

833 Moresco, J.J., and Koelle, M.R. (2004). Activation of EGL-47, a Galpha(o)-coupled receptor, inhibits
834 function of hermaphrodite-specific motor neurons to regulate Caenorhabditis elegans egg-
835 laying behavior. J Neurosci *24*, 8522-8530.
836 Mujica, P.E., and Gonzalez, F.G. (2011). Interaction between IP(3) receptors and BK channels in arterial
837 smooth muscle: non-canonical IP(3) signaling at work. J Gen Physiol *137*, 473-477.
838 Newton, A.C. (2001). Protein kinase C: structural and spatial regulation by phosphorylation, cofactors,
839 and macromolecular interactions. Chem Rev *101*, 2353-2364.
840 Nurrish, S., Segalat, L., and Kaplan, J.M. (1999). Serotonin inhibition of synaptic transmission: Galpha(0)
841 decreases the abundance of UNC-13 at release sites. Neuron *24*, 231-242.
842 Oakes, M., Law, W.J., and Komuniecki, R. (2019). Cannabinoids Stimulate the TRP Channel-Dependent
843 Release of Both Serotonin and Dopamine to Modulate Behavior in C. elegans. J Neurosci *39*,
844 4142-4152.
845 Oakes, M.D., Law, W.J., Clark, T., Bamber, B.A., and Komuniecki, R. (2017). Cannabinoids Activate
846 Monoaminergic Signaling to Modulate Key C. elegans Behaviors. J Neurosci *37*, 2859-2869.
847 Offermanns, S. (2001). In vivo functions of heterotrimeric G-proteins: studies in Galpha-deficient mice.
848 Oncogene *20*, 1635-1642.
849 Ohno, H., Sakai, N., Adachi, T., and Iino, Y. (2017). Dynamics of Presynaptic Diacylglycerol in a Sensory
850 Neuron Encode Differences between Past and Current Stimulus Intensity. Cell Rep *20*, 2294-
851 2303.
852 Okochi, Y., Kimura, K.D., Ohta, A., and Mori, I. (2005). Diverse regulation of sensory signaling by C.
853 elegans nPKC-epsilon/eta TTX-4. EMBO J *24*, 2127-2137.

854 Pastuhov, S.I., Matsumoto, K., and Hisamoto, N. (2016). Endocannabinoid signaling regulates
855 regenerative axon navigation in Caenorhabditis elegans via the GPCRs NPR-19 and NPR-32.
856 Genes Cells *21*, 696-705.
857 Porter, M.Y., and Koelle, M.R. (2010). RSBP-1 is a membrane-targeting subunit required by the
858 Galpha(q)-specific but not the Galpha(o)-specific R7 regulator of G protein signaling in
859 Caenorhabditis elegans. Mol Biol Cell *21*, 232-243.
860 Ravi, B., Garcia, J., and Collins, K.M. (2018a). Homeostatic Feedback Modulates the Development of
861 Two-State Patterned Activity in a Model Serotonin Motor Circuit in Caenorhabditis elegans.
862 J Neurosci *38*, 6283-6298.
863 Ravi, B., Nassar, L.M., Kopchock, R.J., 3rd, Dhakal, P., Scheetz, M., and Collins, K.M. (2018b).
864 Ratiometric Calcium Imaging of Individual Neurons in Behaving Caenorhabditis Elegans. J Vis
865 Exp.
866 Ravi, B., Zhao, J., Chaudhry, S., Bartole, M., Kopchock, R.J., Guijarro, C., Kang, L., and Collins, K.M.
867 (2020). Presynaptic Gα_o (GOA-1) signals to depress command neuron
868 excitability and allow stretch-dependent modulation of egg laying in Caenorhabditis
869 elegans. bioRxiv, 701664.
870 Reynolds, N.K., Schade, M.A., and Miller, K.G. (2005). Convergent, RIC-8-dependent Galpha signaling
871 pathways in the Caenorhabditis elegans synaptic signaling network. Genetics *169*, 651-670.
872 Rojas, R.J., Yohe, M.E., Gershburg, S., Kawano, T., Kozasa, T., and Sondek, J. (2007). Galphaq directly
873 activates p63RhoGEF and Trio via a conserved extension of the Dbl homology-associated
874 pleckstrin homology domain. J Biol Chem *282*, 29201-29210.
875 Rose, A.M., and Baillie, D.L. (1980). Genetic organization of the region around UNC-15 (I), a gene
876 affecting paramyosin in Caenorhabditis elegans. Genetics *96*, 639-648.

877 Rozengurt, E., Sinnett-Smith, J., and Zugaza, J.L. (1997). Protein kinase D: a novel target for
878 diacylglycerol and phorbol esters. Biochem Soc Trans *25*, 565-571.
879 Seifert, J.P., Zhou, Y., Hicks, S.N., Sondek, J., and Harden, T.K. (2008). Dual activation of phospholipase
880 C-epsilon by Rho and Ras GTPases. J Biol Chem *283*, 29690-29698.
881 Shimizu, T., Pastuhov, S.I., Hanafusa, H., Matsumoto, K., and Hisamoto, N. (2018). The C. elegans
882 BRCA2-ALP/Enigma Complex Regulates Axon Regeneration via a Rho GTPase-ROCK-MLC
883 Phosphorylation Pathway. Cell Rep *24*, 1880-1889.
884 Shyn, S.I., Kerr, R., and Schafer, W.R. (2003). Serotonin and Go modulate functional states of neurons
885 and muscles controlling C. elegans egg-laying behavior. Curr Biol *13*, 1910-1915.
886 Sieburth, D., Madison, J.M., and Kaplan, J.M. (2007). PKC-1 regulates secretion of neuropeptides. Nat
887 Neurosci *10*, 49-57.
888 Silinsky, E.M., and Searl, T.J. (2003). Phorbol esters and neurotransmitter release: more than just
889 protein kinase C? Br J Pharmacol *138*, 1191-1201.
890 Simon, M.I., Strathmann, M.P., and Gautam, N. (1991). Diversity of G proteins in signal transduction.
891 Science *252*, 802-808.
892 Soltesz, I., Alger, B.E., Kano, M., Lee, S.H., Lovinger, D.M., Ohno-Shosaku, T., and Watanabe, M. (2015).
893 Weeding out bad waves: towards selective cannabinoid circuit control in epilepsy. Nat Rev
894 Neurosci *16*, 264-277.
895 Stauffer, T.P., Ahn, S., and Meyer, T. (1998). Receptor-induced transient reduction in plasma
896 membrane PtdIns(4,5)P2 concentration monitored in living cells. Curr Biol *8*, 343-346.
897 Steven, R., Kubiseski, T.J., Zheng, H., Kulkarni, S., Mancillas, J., Ruiz Morales, A., Hogue, C.W., Pawson,
898 T., and Culotti, J. (1998). UNC-73 activates the Rac GTPase and is required for cell and
899 growth cone migrations in C. elegans. Cell *92*, 785-795.

900 Steven, R., Zhang, L., Culotti, J., and Pawson, T. (2005). The UNC-73/Trio RhoGEF-2 domain is required
901 in separate isoforms for the regulation of pharynx pumping and normal neurotransmission
902 in C. elegans. Genes Dev *19*, 2016-2029.
903 Tabuse, Y. (2002). Protein kinase C isotypes in C. elegans. J Biochem *132*, 519-522.
904 Tabuse, Y., Nishiwaki, K., and Miwa, J. (1989). Mutations in a protein kinase C homolog confer phorbol
905 ester resistance on Caenorhabditis elegans. Science *243*, 1713-1716.
906 Tanimura, A., Yamazaki, M., Hashimotodani, Y., Uchigashima, M., Kawata, S., Abe, M., Kita, Y.,
907 Hashimoto, K., Shimizu, T., Watanabe, M.*, et al.* (2010). The endocannabinoid 2-
908 arachidonoylglycerol produced by diacylglycerol lipase alpha mediates retrograde
909 suppression of synaptic transmission. Neuron *65*, 320-327.
910 Tanis, J.E., Moresco, J.J., Lindquist, R.A., and Koelle, M.R. (2008). Regulation of serotonin biosynthesis
911 by the G proteins Galphao and Galphaq controls serotonin signaling in Caenorhabditis
912 elegans. Genetics *178*, 157-169.
913 Tewson, P., Westenberg, M., Zhao, Y., Campbell, R.E., Quinn, A.M., and Hughes, T.E. (2012).
914 Simultaneous detection of Ca2+ and diacylglycerol signaling in living cells. PLoS One *7*,
915 e42791.
916 Thomas, J.H. (1990). Genetic analysis of defecation in Caenorhabditis elegans. Genetics *124*, 855-872.
917 Thore, S., Dyachok, O., Gylfe, E., and Tengholm, A. (2005). Feedback activation of phospholipase C via
918 intracellular mobilization and store-operated influx of Ca2+ in insulin-secreting beta-cells. J
919 Cell Sci *118*, 4463-4471.
920 Trent, C., Tsuing, N., and Horvitz, H.R. (1983). Egg-laying defective mutants of the nematode
921 Caenorhabditis elegans. Genetics *104*, 619-647.

922 Vázquez-Manrique, R.P., Nagy, A.I., Legg, J.C., Bales, O.A., Ly, S., and Baylis, H.A. (2008). Phospholipase
923 C-epsilon regulates epidermal morphogenesis in Caenorhabditis elegans. PLoS Genet *4*,
924 e1000043.
925 Waggoner, L.E., Dickinson, K.A., Poole, D.S., Tabuse, Y., Miwa, J., and Schafer, W.R. (2000a). Long-term
926 nicotine adaptation in Caenorhabditis elegans involves PKC-dependent changes in nicotinic
927 receptor abundance. J Neurosci *20*, 8802-8811.
928 Waggoner, L.E., Hardaker, L.A., Golik, S., and Schafer, W.R. (2000b). Effect of a neuropeptide gene on
929 behavioral states in Caenorhabditis elegans egg-laying. Genetics *154*, 1181-1192.
930 Waggoner, L.E., Zhou, G.T., Schafer, R.W., and Schafer, W.R. (1998). Control of alternative behavioral
931 states by serotonin in Caenorhabditis elegans. Neuron *21*, 203-214.
932 Wettschureck, N., van der Stelt, M., Tsubokawa, H., Krestel, H., Moers, A., Petrosino, S., Schütz, G., Di
933 Marzo, V., and Offermanns, S. (2006). Forebrain-specific inactivation of Gq/G11 family G
934 proteins results in age-dependent epilepsy and impaired endocannabinoid formation. Mol
935 Cell Biol *26*, 5888-5894.
936 White, J.G., Southgate, E., Thomson, J.N., and Brenner, S. (1986). The structure of the nervous system
937 of the nematode Caenorhabditis elegans. Philos Trans R Soc Lond B Biol Sci *314*, 1-340.
938 Wilkie, T.M., Gilbert, D.J., Olsen, A.S., Chen, X.N., Amatruda, T.T., Korenberg, J.R., Trask, B.J., de Jong,
939 P., Reed, R.R., Simon, M.I.*, et al.* (1992). Evolution of the mammalian G protein alpha
940 subunit multigene family. Nat Genet *1*, 85-91.
941 Williams, S.L., Lutz, S., Charlie, N.K., Vettel, C., Ailion, M., Coco, C., Tesmer, J.J., Jorgensen, E.M.,
942 Wieland, T., and Miller, K.G. (2007). Trio's Rho-specific GEF domain is the missing Galpha q
943 effector in C. elegans. Genes Dev *21*, 2731-2746.

944 Wing, M.R., Snyder, J.T., Sondek, J., and Harden, T.K. (2003). Direct activation of phospholipase C-
945 epsilon by Rho. J Biol Chem *278*, 41253-41258.
946 Xiao, H., Hapiak, V.M., Smith, K.A., Lin, L., Hobson, R.J., Plenefisch, J., and Komuniecki, R. (2006). SER-1,
947 a Caenorhabditis elegans 5-HT2-like receptor, and a multi-PDZ domain containing protein
948 (MPZ-1) interact in vulval muscle to facilitate serotonin-stimulated egg-laying. Dev Biol *298*,
949 379-391.
950 Xiao, L., Eto, M., and Kazanietz, M.G. (2009). ROCK mediates phorbol ester-induced apoptosis in
951 prostate cancer cells via p21Cip1 up-regulation and JNK. J Biol Chem *284*, 29365-29375.
952 Yang, L., Dai, F., Tang, L., Le, Y., and Yao, W. (2017). Macrophage differentiation induced by PMA is
953 mediated by activation of RhoA/ROCK signaling. J Toxicol Sci *42*, 763-771.
954 Yu, H., Aleman-Meza, B., Gharib, S., Labocha, M.K., Cronin, C.J., Sternberg, P.W., and Zhong, W. (2013).
955 Systematic profiling of Caenorhabditis elegans locomotive behaviors reveals additional
956 components in G-protein Galphaq signaling. Proc Natl Acad Sci U S A *110*, 11940-11945.
957